NAVAL POSTGRADUATE SCHOOL
MONTEREY, CALIFORNIA 93943-5002

NAVAL POSTGRADUATE SCHOOL
Monterey, California

THESIS

A MARITIME AND CONTINENTAL AEROSOL-CLOUD INTERACTION STUDY FROM ASTEX '92

by

Karen M. Ruppe

December, 1992

Thesis Advisor: Philip A. Durkee

Approved for public release; distribution is unlimited.

T258505

REPORT DOCUMENTATION PAGE

1a Report Security Classification: Unclassified		1b Restrictive Markings	
2a Security Classification Authority		3 Distribution/Availability of Report	
2b Declassification/Downgrading Schedule		Approved for public release; distribution is unlimited.	
4 Performing Organization Report Number(s)		5 Monitoring Organization Report Number(s)	
6a Name of Performing Organization Naval Postgraduate School	6b Office Symbol *(if applicable)*	7a Name of Monitoring Organization Naval Postgraduate School	
6c Address *(city, state, and ZIP code)* Monterey CA 93943-5000		7b Address *(city, state, and ZIP code)* Monterey CA 93943-5000	
8a Name of Funding/Sponsoring Organization	6b Office Symbol *(if applicable)*	9 Procurement Instrument Identification Number	
Address *(city, state, and ZIP code)*		10 Source of Funding Numbers	
		Program Element No / Project No / Task No / Work Unit Accession No	

11 Title *(include security classification)* A MARITIME AND CONTINENTAL AEROSOL-CLOUD INTERACTION STUDY FROM ASTEX '92

12 Personal Author(s) Ruppe, Karen M.

13a Type of Report	13b Time Covered From To	14 Date of Report *(year, month, day)*	15 Page Count
Master's Thesis			114

16 Supplementary Notation The views expressed in this thesis are those of the author and do not reflect the official policy or position of the Department of Defense or the U.S. Government.

17 Cosati Codes			18 Subject Terms *(continue on reverse if necessary and identify by block number)*
Field	Group	Subgroup	satellite cloud analysis, cloud distribution, aerosol distribution, aerosol classification

19 Abstract *(continue on reverse if necessary and identify by block number)*

Variations in marine stratocumulus microphysics during FIRE IFO 1992 are observed and analyzed through the use of NOAA 10/11/12 AVHRR satellite data. Maritime and continental aerosols in clear-air and cloudy regions are characterized by particle size index, optical depth, and low cloud analysis at visible and 3.7 μm wavelengths. Use of satellite-detected radiances to resolve aerosol type and distribution prove useful in determining implications of cloud reflectance changes due to modification by aerosol particles. Air masses were clearly defined and showed distinctive signatures in aerosol characteristics and cloud reflectances at 3.7 μm wavelengths. Air mass characteristic sources consisted of industrial aerosols out of Europe and desert dust from the Sahara Desert.

20 Distribution/Availability of Abstract	21 Abstract Security Classification	
__ unclassified/unlimited __ same as report __ DTIC users	Unclassified	
22a Name of Responsible Individual Durkee, Philip A.	22b Telephone *(include Area Code)* 408-656-3465	22c Office Symbol MR/De

DD FORM 1473,84 MAR 83 APR edition may be used until exhausted — security classification of this page

All other editions are obsolete — Unclassified

Approved for public release; distribution is unlimited.

A Maritime and Continental Aerosol-Cloud Interaction Study From ASTEX '92

by

Karen M. Ruppe
Lieutenant, United States Naval Reserve
B.A., University of Virginia, 1978
M.S., Old Dominion University, 1981

Submitted in partial fulfillment
of the requirements for the degree of

MASTER OF SCIENCE IN METEOROLOGY AND PHYSICAL OCEANOGRAPHY

from the

NAVAL POSTGRADUATE SCHOOL
December 1992

ABSTRACT

Variations in marine stratocumulus microphysics during FIRE IFO 1992 are observed and analyzed through the use of NOAA 10/11/12 AVHRR satellite data. Maritime and continental aerosols in clear-air and cloudy regions are characterized by particle size index, optical depth, and low cloud analysis at visible and 3.7 μm wavelengths. Use of satellite-detected radiances to resolve aerosol type and distribution prove useful in determining implications of cloud reflectance changes due to modification by aerosol particles. Air masses were clearly defined and showed distinctive signatures in aerosol characteristics and cloud reflectances at 3.7 μm wavelengths. Air mass characteristic sources consisted of industrial aerosols out of Europe and desert dust from the Sahara Desert.

R887
C.1

TABLE OF CONTENTS

I. INTRODUCTION 1
A. PURPOSE 1
B. THE FIRST ISCCP REGIONAL EXPERIMENT PHASE II . 2
C. MOTIVATION 5
1. Climatological 5
2. Military 6

II. THEORY 7
A. RADIATIVE PROCESSES 7
B. CONTINENTAL AND MARITIME AEROSOL CHARACTERISTICS 8
1. Continental Aerosols 8
a. Desert Aerosols - 8
b. Clean-Continental Aerosols - 9
c. Average-Continental Aerosols - 9
2. Maritime Aerosols 9
a. Clean-maritime Aerosols 9
b. Maritime-mineral Aerosols 10
C. PARAMETERS USED FOR CONTINENTAL VERSUS MARITIME AEROSOL STUDY 10
1. Aerosol Particle Size Index (S12) 10
2. Optical Depth 11

DUDLEY KNOX LIBRARY
NAVAL POSTGRADUATE SCHOOL
MONTEREY, CALIFORNIA 93943-5002

3. LOW1 13
4. LOW3 13

III. PROCEDURES 15
A. DATA RETRIEVAL 15
B. DATA PROCESSING 15
1. Initial Data Tape Processing 16
2. Subscene Processing 16
3. Track Identification and Sampling 16

IV. CASE STUDY RESULTS AND EVALUATION 18
A. FIRE IFO 1992 CASE STUDY 19
1. CSD1 (14 June, 1992) 19
a. Synoptic Summary 19
b. Satellite Interpretation 20
c. Cross-section Results 21
(1) Optical Depth (TTHG) 21
(2) S12 Values 21
(3) LOW1 22
(4) LOW3 22
2. CSD2 (15 June, 1992) 23
a. Synoptic Summary 23
b. Satellite Interpretation 36
c. Cross-section Results 37
(1) Optical Depth (TTHG) 37
(2) S12 37

(3) LOW1 37
(4) LOW3 38
3. CSD3 (16 June, 1992) 38
a. Synoptic Summary 38
b. Satellite Interpretation 51
c. Cross-section Results 52
(1) LOW1 52
(2) LOW3 53
4. CSD4 (17 June, 1992) 54
a. Synoptic Summary 54
b. Satellite Interpretation 54
c. Cross-section results 67
(1) LOW1 67
(2) LOW3 68
5. CSD5 (18 June, 1992) 69
a. Synoptic Summary 69
b. Satellite Interpretation 82
c. Cross-section Results 82
(1) LOW1 82
(2) LOW3 83
B. CASE STUDY CONCLUSIONS 83

V. CONCLUSIONS AND RECOMMENDATIONS 96
A. CONCLUSIONS 96
B. RECOMMENDATIONS 98

LIST OF REFERENCES 99

INITIAL DISTRIBUTION LIST 101

LIST OF FIGURES

Figure 1. Geographical Chart of the Madeira Region . . 4

Figure 2. Surface Pressure Chart valid 1200 UTC 14JUN92 24

Figure 3. 14JUN92 Back Trajectories Within the Project Region: (a) 700mb and (b) 1000mb 25

Figure 4a. LOW1 Satellite Image of 090330 UTC 14JUN92 . 26

Figure 4b. LOW 1 Satellite Image of 162530 UTC 14JUN92 27

Figure 5a. LOW3 Satellite Image of 090330 UTC 14JUN92 . 28

Figure 5b. LOW3 Satellite Image of 162530 UTC 14JUN92 . 29

Figure 6. Parameter Results from 090330 UTC 14JUN92: Track A 30

Figure 7. Parameter Results from 090330 UTC 14JUN92: Track B 31

Figure 8. Parameter Results from 090330 UTC 14JUN92: Track C 32

Figure 9. Parameter Results from 162530 UTC 14JUN92: Track A 33

Figure 10. Parameter Results from 162530 UTC 14JUN92: Track B 34

Figure 11. Parameter Results from 162530 UTC 14JUN92: Track C 35

Figure 12. Surface Pressure Chart Valid 1200 UTC 15JUN92 39

Figure 13. 15JUN92 Back-Trajectories Within the Project

Region: (a) 700mb and (b) 1000mb 40
Figure 14a. LOW1 Satellite Image of 084200 UTC 15JUN92 41
Figure 14b. LOW1 Satellite Image of 161330 UTC 15JUN92 42
Figure 15a. LOW3 Satellite Image of 084200 UTC 15JUN92 43
Figure 15b. LOW3 Satellite Image of 161330 UTC 15JUN92 44
Figure 16. Parameter Results from 084200 UTC 15JUN92:
Track A 45
Figure 17. Parameter Results from 084200 UTC 15JUN92:
Track B 46
Figure 18. Parameter Results from 084200 UTC 15JUN92:
Track C 47
Figure 19. Parameter Results from 161330 UTC 15JUN92:
Track A 48
Figure 20. Parameter Results from 161330 UTC 15JUN92:
Track B 49
Figure 21. Parameter Results from 161330 UTC 15JUN92:
Track C 50
Figure 22. Surface Pressure Chart Valid 1200 UTC
16JUN92 55
Figure 23. 16JUN92 Back Trajectories Within the Project
Region: (a) 700mb and (b) 1000mb 56
Figure 24a. LOW1 Satellite Image of 095900 UTC 16JUN92 57
Figure 24b. LOW1 Satellite Image of 160130 UTC 16JUN92 58
Figure 25a. LOW3 Satellite Image of 095900 UTC 16JUN92 59
Figure 25b. LOW3 Satellite Image of 160130 UTC 16JUN92 60
Figure 26. Parameter Results from 095900 UTC 16JUN92:

Track A 61
Figure 27. Parameter Results from 095900 UTC 16JUN92:
Track B 62
Figure 28. Parameter Results from 095900 UTC 16JUN92:
Track C 63
Figure 29. Parameter Results from 160130 UTC 16JUN92:
Track A 64
Figure 30. Parameter Results from 160130 UTC 16JUN92:
Track B 65
Figure 31. Parameter Results from 160130 UTC 16JUN92:
Track C 66
Figure 32. Surface Pressure Chart Valid 1200 UTC 17JUN92
. 70
Figure 33. 17JUN92 Back Trajectories Within the Project
Region: (a) 700mb and (b) 1000mb 71
Figure 34a. LOW1 Satellite Image of 093900 UTC 17JUN92 72
Figure 34b. LOW1 Satellite Image of 154930 UTC 17JUN92 73
Figure 35a. LOW3 Satellite Image of 093900 UTC 17JUN92 74
Figure 35b. LOW3 Satellite Image of 154930 UTC 17JUN92 75
Figure 36. Parameter Results from 093900 UTC 17JUN92:
Track A 76
Figure 37. Parameter Results from 093900 UTC 17JUN92:
Track B 77
Figure 38. Parameter Results from 093900 UTC 17JUN92:
Track C 78
Figure 39. Parameter Results from 154930 UTC 17JUN92:

Track A 79
Figure 40. Parameter Results from 154930 UTC 17JUN92: Track B 80
Figure 41. Parameter Results from 154930 UTC 17JUN92: Track C 81
Figure 42. Surface Pressure Chart Valid 1200 UTC 18JUN92 84
Figure 43. 18JUN92 Back Trajectories Within the Project Region: (a) 700mb and (b) 1000mb 85
Figure 44. LOW1 Satellite Image of 153745 UTC 18JUN92 . 86
Figure 45. LOW3 Satellite Image of 153745 UTC 18JUN92 . 87
Figure 46. Parameter Results from 153745 UTC 18JUN92: Track A 88
Figure 47. Parameter Results from 153745 UTC 18JUN92: Track B 89
Figure 48. Parameter Results from 153745 UTC 18JUN92: Track C 90
Figure 49. Continental (dashed) and Maritime (solid) Air Mass Motion for 14JUN92 - 17JUN92 93
Figure 50. Average Optical Depth and S12 Value Plots 14JUN92 - 16JUN92 94
Figure 51. Marine versus Continental LOW1 and LOW3 Values 14JUN92 - 18JUN92 95

ACKNOWLEDGMENTS

I would like to thank Mr. Kurt Nielsen, Mr. Chuck Skupniewicz, and Mr. Craig Motell for their invaluable programming skills and problem-solving assistance. They spent endless hours adapting dat tapes to the Naval Postgraduate School's computer system and wrote programs enabling more rapid resolution of the data. Dr. Pat Pauley provided expertise in satellite imagery cloud interpretation, and her patience and time are very much appreciated. I would most especially like to express my thanks and appreciation to Dr. Phil Durkee for his patience and encouragement throughout this study, and for being the instrument for maintaining high levels of morale during our stay in the Azores!

I. INTRODUCTION

A. PURPOSE

Understanding the mechanisms which affect climate changes are paramount if we expect to maintain a healthy environment on our planet. One tool available for studying these mechanisms is remote sensing, which offers the unique opportunity to observe and sample atmospheric constituents on a global scale. Of particular interest is the measurement of aerosols and their effect on clear and cloudy regions.

Aerosols can be divided into 6 categories based on origin: clean (continental or rural, forest, maritime, and polar), average continental, desert (background and wind-carrying dust), urban or industrial, maritime (mineral and polluted) and polar polluted (d'Almeida et al. 1991). The effects of man-made aerosols and pollutants drastically affect the climate by providing large numbers of smaller aerosols to the lower atmosphere. The scattering and absorption by clouds and aerosol particles influence the earth's radiation budget and therefore effect climatological change. As continental aerosols are transported over water basins, they eventually interact with maritime aerosols forming a more complex air mass (which has been modified by a combination of particle types). The scattering and absorption characteristics of

these aerosols are distinctive and can be detected by their radiance signatures via satellite.

The primary objective of this thesis is to use data collected during phase II of FIRE [First ISCCP (International Satellite Cloud Climatology Project) Regional Experiment] to qualitatively identify maritime and continental aerosols present in cloud-free and stratocumulus regions, thus substantiating a similar study done by Mineart (1988) off coastal California. Specifically, classification will be accomplished through the use of radiance signatures via satellites, air mass trajectories, aerosol size distribution and by-products of the satellite data.

B. THE FIRST ISCCP REGIONAL EXPERIMENT PHASE II

FIRE is an ongoing multi-agency program designed to enhance and improve the development of cloud and radiation parameterizations for integration into climate models, and to provide for evaluation and improvement of the products of ISCCP. The scientific objectives of FIRE Phase II, outlined in the ASTEX (1990) are to:

- Expand basic knowledge of how clouds and cloud systems interact with their environment and the climate;
- Identify, quantify, and simulate processes instrumental in the evolution of large-scale cloud systems;
- Quantify the capabilities of current models and improve the cloudiness and radiation parameterizations used in Global Climate Models (GCM);
- Improve the capabilities of current models to effectively

simulate large-scale cloud systems;

- Assess and improve the reliability of currently used cloud/radiation monitoring systems (both locally and remotely); and
- Assess the capability of future monitoring systems such as the Earth Observing System (EOS).

The data for this thesis were collected during the second marine stratocumulus intensive field observations (IFO) conducted from 1 June to 1 July, 1992 in the eastern North Atlantic. The mission, titled project ASTEX (Atlantic Stratocumulus Transition Experiment) was located within an eastern Atlantic region extending southeast from Santa Maria (37N25W) in the Azores to Porto Santo (33N16W), a small island just north of Madeira (triangle in Figure 1). The study included surface measurements, aircraft operations, and shipboard oceanographic investigations. A variety of meteorological and oceanographic upper air and surface measurements were conducted and included two constant-altitude balloon lagrangian experiments which probed air parcel modification along the base of the Marine Atmospheric Boundary Layer (MABL), a microwave radiometer, a Doppler wind profiler, sodar and radar, rawinsonde releases from Santa Maria, remote sensors, and a collection of standard instrumentation for measurements of temperature, moisture, heat flux, irradiance, etc. Seven aircraft participated in ASTEX: a National Aeronautics and Space Administration (NASA) DC-8, the University of Washington C-131A, the National Center for

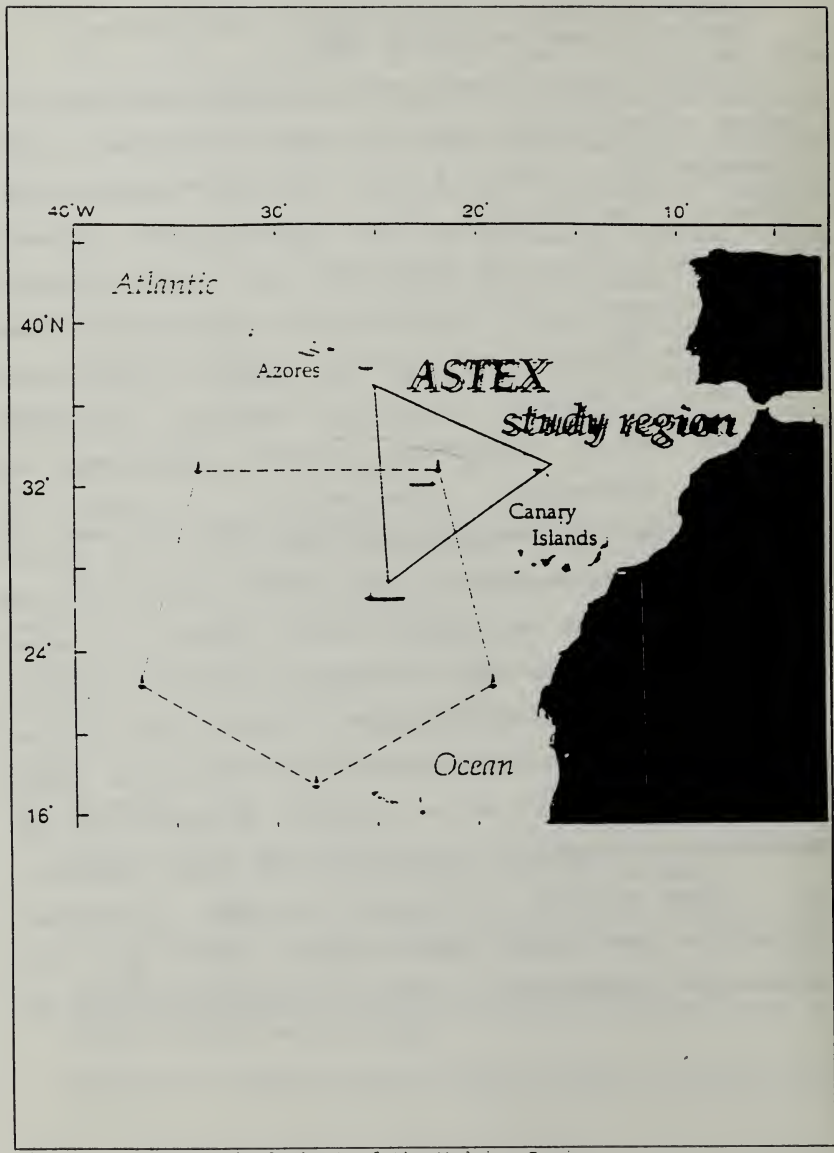

Figure 1. Geographical Chart of the Madeira Region

Atmospheric Research (NCAR) Electra, a C-130 operated by the British Meteorological Office, a United States Navy P-3, a ARAT Fokker F-27 French aircraft operated as part of the Surface of the Ocean, Fluxes and Interactions with the Atmosphere (SOFIA) experiment, and a Merlin IV aircraft operated by the French Meteorological Office. Four ships, the NOAA ship *Malcolm Baldridge*, the *Oceanus* from Woods Hole, Massachusetts, the German ship *Valdevia*, and the French ship *Le Suroit* also participated. The individual capabilities of these platforms as well as other ground and satellite-based systems are described in NASA (1990).

The satellite data used in this thesis are from NOAA polar orbiting platforms (NOAA-10/11/12) Advanced Very High Resolution Radiometers (AVHRR) collected on station at Santa Maria during ASTEX. Data for use in trajectory analyses are provided by Chris Bretherton of the University of Washington. Synoptic summaries are derived from a combination of National Meteorological Center (NMC) analyses and observed weather patterns during ASTEX.

C. MOTIVATION

There are two motivational initiatives for this study: climatological and military.

1. Climatological

The earth's radiation budget is based on incoming and outgoing radiation as a function of time and space. Aerosols

are suspended solid or liquid particles dispersed in the atmosphere that act as scattering or absorbing centers for the incoming and/or outgoing radiation. As industries developed over historical time, so too did the by-products of industry, namely the pollutants released into the atmosphere, e.g., soot, smoke, radioactive fallout, etc. The increase in man-made aerosols has acted to alter the earth's radiation budget (Charlson, et al. 1987) and has played a role in such controversial issues as the "Greenhouse Effect" (a warming of the earth's climate due to trapped outgoing long wave radiation) as well as the earth's possible cooling due to a buildup of aerosols (McCormick and Ludwig, 1967).

2. Military

The presence of different types of aerosols presents potential problems in the use of electro-optical devices for military and commercial application. For example, the optimum wavelength region for laser systems is between .4 and 1.0 μm (Bloembergen et al. 1987). Aerosols are characterized as being 1 micron or less in diameter and act as strong contributors of energy loss to the lasers in the .4 - 1.0 μm band.

Therefore, the ability to categorize aerosols is an asset in determining optimum equipment capabilities for military and commercial applications and could also identify aerosol origins and their impact on the earth's radiation budget.

II. THEORY

A. RADIATIVE PROCESSES

Radiant energy propagating through the earth's atmosphere is scattered and/or absorbed by interactions with solid, liquid, and gaseous particles as well as clouds and the surface of the earth. This attenuation is dependent upon electromagnetic wavelengths and atmospheric constituents. AVHRR satellites measure wavelength bands in five channels, each exploiting an atmospheric absorption "window" where the incoming radiant energy is primarily affected by scattering only. Table 1 shows the specific bandwidths for channels 1 - 5.

Table 1. AVHRR Channel Bandwidth (Kidwell, 1986)

	Radiance	Bandwidth (μm)
1	Visible	.58 - .68
2	Red/Near IR	.70 - 1.10
3	Thermal IR	3.50 - 3.90
4	Thermal IR	10.30 - 11.50
5	Thermal IR	11.30 - 12.40

Use of the scattered solar energy measured by AVHRR satellites provides a means of measuring various properties of aerosols including optical depth, particle size index, low-level radiance, and particle distribution. This is dependent on the scattering ability of the suspended aerosols contained in the atmosphere.

Scattered solar energy received from clouds and particles contained within the cloud are sensitive to all wavelengths (vice the short wavelength sensitivity of aerosols). Wavelength dependence differs due to differences in particle sizes contained within the cloud.

B. CONTINENTAL AND MARITIME AEROSOL CHARACTERISTICS

1. Continental Aerosols

Continental aerosols of natural and industrial origin are present in the tropopause and can mix downward into the upper portions of the marine atmospheric boundary layer (MABL) as they are transported above the marine layer by upper level flow patterns.

Continental aerosols possibly present within the ASTEX region include:

a. Desert Aerosols -

Present in the Sahara Desert and transported by favorable meteorological conditions into the eastern Atlantic;

b. Clean-Continental Aerosols -

Consisting of dust-like and water-soluble substances encountered in remote, pollution-free, and continental areas such as rural environments; and

c. Average-Continental Aerosols -

Consisting of the type of airborne particulate matter in regions from remote polluted locations (such as western Europe) influenced by industrial activity, traffic, and other anthropogenic activities leading to aerosol introduction.

2. Maritime Aerosols

Maritime aerosols are plentiful around the world as the oceans account for about two-thirds of the earth's surface and constitute the major sources of sea-salt and biogenic particles released or formed in the atmosphere. They are present near the surface and in the lower MABL as particles are lifted by synoptic patterns in the lower atmosphere. The maritime aerosols possible in the ASTEX region include:

a. Clean-maritime Aerosols

Aerosols produced above oceanic areas of remote maritime environments (such as islands) and made up of biogenically produced sulfates (NSS or non-sea-salt sulfates) and sea-salt particles; and

b. Maritime-mineral Aerosols

A mixture of desert aerosols with particles of maritime origin. These aerosol types would be present within the MABL with desert aerosols in the upper boundary layer (transported from above) and maritime aerosols in the lower portions of the boundary layer (closer to marine origins).

In general, addition of aerosol particles produces increases in the number of cloud condensation nucleii (CCN) and cloud droplets, and ultimately decreases individual droplet size in clouds (through droplet interaction). Maritime aerosols tend to have fewer aerosols per unit volume and, with fewer CCN present, clouds are characterized by larger droplet sizes (Mineart,1988).

C. PARAMETERS USED FOR CONTINENTAL VERSUS MARITIME AEROSOL STUDY

1. Aerosol Particle Size Index (S12)

The relationship between radiance and aerosol size distribution is characterized by the aerosol particle size index. Durkee (1984) showed that aerosol-particle-dependent terms of the radiative transfer equation (RTE) are larger at channel 1 (red) wavelengths than at channel 2 (near infrared) wavelengths, and are correlated with aerosol optical depth. Since satellite-detected radiances are proportional to the aerosol-particle-dependent terms, variations in radiance will

result from variations in aerosol-particle-dependent terms. The aerosol particle size index ratio is defined as

$$S12 = \frac{(L_A)_{red}}{(L_A)_{nir}} \approx \frac{(\delta_A)_{red}}{(\delta_A)_{nir}} \quad (1)$$

where L_A = aerosol radiance

δ_A = optical depth due to aerosol particles, defined as

$$\delta_A = \frac{(L_A\ 4\ \mu)}{(\omega_0\ F_0\ p(\phi))}$$

where ω_0 = single scatter albedo

$\mu = \cos(\theta)$ (observation zenith angle)

$p(\phi)$ = scattering phase function

F_0 = solar radiative flux

In general, the greater the contribution of smaller particles, the larger the ratio. This is because larger numbers of smaller particles display a significantly greater difference between channel 1 and channel 2 reflectances (with channel 1 dominating) than do the same number of larger particles. Therefore, continental aerosols should depict a larger S12 value than maritime aerosols.[1]

2. Optical Depth

Optical depth is the sum of the extinction coefficient from the surface to satellite altitude (Durkee, 1984):

[1]Miller (1991) and Clifford (1991) addresses inflated S12 index values due to the presence of water vapor. Their improvements and modifications to s12 measurements are incorporated, as applicable, for ASTEX measurements.

$$\delta = \int_0^H \beta_{ext}\, dz, \qquad (2)$$

where H = height

β_{ext} = extinction coefficient

When the optical depth is linked to the particle size and distribution of aerosol particles (as in clear-air regions), it is possible to correlate the satellite-detected radiance with size distributions of aerosols present. Since β_{ext} is a function of the aerosol particle size and distribution, and the optical depth is a function of β_{ext}, changes in aerosol particle size and/or distribution will be reflected in changes of optical depth and satellite-detected radiance.

The Two-Term Henyey-Greenstein (TTHG) variable phase function was used to examine the optical depth for this study. The scattering phase function describes that fraction of radiation scattered in a given direction; however, one single phase function does not adequately express the optical depth for all aerosol distributions. The TTHG addresses this problem by using a variable phase function (Lenoble, 1985):

$$p(\theta) = \frac{\alpha\,(1 - g_1^2)}{(1 + g_1^2) - 2\,g_1 \cos(\theta))} + \frac{(1 - \alpha)\,(1 - g_2^2)}{(1 + g_2^2 + 2\,g_2 \cos(\theta))}, \qquad (3)$$

where α = weighting factor

g_1, g_2 = asymmetry curve factors

The asymmetry curve factors in equation (3) are S12 sensitive and therefore, as S12 varies, the phase function varies and so does optical depth (Durkee, et al. 1991).

At a given wavelength, an increase in particle size distribution will cause a decrease in the number of particles per unit volume, which will interact to decrease the radius sizes and produce an overall increase in scatter and therefore optical depth. When comparing an air parcel of continental versus maritime aerosol composition it is expected that continental parcel will have a greater optical depth due to the greater number of smaller drops per unit volume.

3. LOW1

LOW1 is a Channel 1 (visible) albedo of low clouds scaled by the solar zenith angle and a low cloud asymmetry reflectance factor. LOW1 is droplet-number sensitive, such that thicker clouds or air parcels will be represented by higher reflectance values.

4. LOW3

LOW3 is a Channel 3 (thermal infrared) albedo of low clouds scaled by the solar zenith angle and a low cloud anisotropic reflectance factor. This basically removes emitted radiance from the 3.7 μm wavelength, leaving the reflected radiance only. LOW3 is droplet-size sensitive and, as such, increased values of LOW3 radiation indicate smaller droplet sizes (increases in the number of aerosols per unit

volume cause increases in CCN which increase the number of droplets and ultimately decrease droplet sizes within the cloud due to droplet interaction) and are more indicative of a continental vice maritime aerosol source.

III. PROCEDURES

A. DATA RETRIEVAL

Satellite passes were collected on station in Santa Maria, Azores using the Naval Postgraduate School's satellite ground station equipment consisting of:

- A Telonics polar satellite tracker and receiver unit;
- A first-order filtering data collector; and
- A workstation for processing the raw satellite data.

Receiving stations collected a total of 137 passes from NOAA satellites 10, 11, and 12. Due to the degraded channel 3 reception of NOAA-10, only NOAA-11 and 12 satellites were processed for this study.

After passes were collected and stored on the workstation computer, they were copied onto 4 millimeter dat tapes for storage and further study.

B. DATA PROCESSING

Processing of satellite data was performed at the U. S. Naval Postgraduate School's Interactive Digital Environmental Analysis (IDEA) Laboratory. The multi-channel analysis routine used in this thesis is a FORTRAN software package run on the IDEA Lab computer system. The following describes the processing steps of this study.

1. Initial Data Tape Processing

In order to access and manipulate the satellite images, the data tapes must initially be gleaned. This process reads raw satellite data and formats it through calibration and navigation such that images can be produced. Once gleaned, the pass is available to the VAX workstation for further processing.

2. Subscene Processing

Sixteen satellite passes were processed for the 14-18 June, 1992 case study. After selecting a subscene from the entire pass that incorporated the ASTEX project region, the following images were promulgated:

- Channels 2, 3, and 4
- LOW1
- LOW3
- TTHG/Optical Depth
- S12

The visual and IR images enabled a general overview of cloud patterns and development in the project area. The LOW1, LOW3, and TTHG images were further studied to determine aerosol characteristics of cloud-free and stratocumulus regions.

3. Track Identification and Sampling

S12 and TTHG images were further studied by selecting regions characterized by the cloud-free region of interest,

with the maritime and continental cloud regimes lying to either side. LOW1 and LOW3 images were used to study the cloud regimes. Three tracks were selected: northern, central, and southern (referred to as Tracks A, B, and C respectively). The pixel and product values of the LOW1, LOW3, S12, and TTHG parameters along these tracks were extracted and transferred into numerical format which was then available for plotting. In order to eliminate the possibility of inconsistencies in the data, a random satellite pass was selected (084200 UTC 15 JUN 92) and intensively studied using 26 non-overlapping tracks. The plotted results showed little or no variability in the parameter data from track to track, with generally the same magnitudes throughout. This shows that data collected from the three selected tracks used in this study are representative of the northern, central, and southern regions of the project area.

IV. CASE STUDY RESULTS AND EVALUATION

This chapter describes the case study period between 14 June, 1992 and 18 June, 1992. Each study day is evaluated synoptically based on satellite imagery, surface and upper level charts, back trajectories of both surface and 700 millibar (mb) air parcels, with an additional section discussing AVHRR subscene results of optical depth, S12, LOW1, and LOW3 values. The case study will be delineated as follows:

Case Study Day 1 (CSD1): Julian Day 166, 14 June, 1992

Case Study Day 2 (CSD2): Julian Day 167, 15 June, 1992

Case Study Day 3 (CSD3): Julian Day 168, 16 June, 1992

Case Study Day 4 (CSD4): Julian Day 169, 17 June, 1992

Case Study Day 5 (CSD5): Julian Day 170, 18 June, 1992

The synoptic features of each day are addressed in order to identify general advective patterns present within the region which substantiate the maritime and continental origins of the air masses. Satellite images presented in this chapter consist of LOW1 and LOW3 visual and IR reflectances and will be specifically studied using 3 cross-sectional areas in the northern, central, and southern portions of the project area (referred to as Tracks A, B, and C respectively). These cross-sectional areas will be evaluated for LOW1, LOW3,

optical depth, and S12 parameters in an effort to qualitatively characterize the air masses present.

Because optical depth interpretation depends upon measurements from the surface to the satellite and S12 is directly related to optical depth measurements (see Chapter II), only cloud-free regions will be sampled for optical depth and S12 parameters. LOW1 and LOW3, which are sensitive to numbers and droplet sizes respectively, are only valid within cloudy regions and will only be sampled in those areas.

Optical depth values obtained through use of satellite imagery appear to be much lower than expected in aerosol rich regions. Since visible satellite channels degrade with time, it is likely that there are calibration errors in the optical depth readings. Therefore, optical depth estimates will be reported as the change in optical depth across the selected track regions.

A. FIRE IFO 1992 CASE STUDY

1. CSD1 (14 June, 1992)

a. Synoptic Summary

At 500mb (not shown), a weak shortwave and developing vortex lie west of the Azores with an upper-level ridge pattern beginning to become apparent, extending northeast to southwest along a line from 54N5W to 30N60W. The combination of this ridge and an existing frontal system over the central coast of Portugal bring a northeasterly surface

flow pattern to the project region (Figure 2). Figure 3a shows that air parcels over the western operating area at the 700mb level are transported from a maritime regime, with the eastern and central portions originating from the United Kingdom region. Figure 3b indicates that at the surface, the maritime air is being advected into the region of continental air in the central portion of the project area.

b. Satellite Interpretation

Figures 4a and b LOW1 images show a developing region in the northwest quadrant consisting of cumuliform and stratiform clouds. There is a distinct boundary of cloud masses (extending north-south along the eastern boundary of the maritime region) which appears to define the extent of maritime air mass influence. The central region consists of a relatively cloud-free area being advected westward from the Iberian Peninsula. The continental air mass is characterized by widely scattered stratocumuliform and cumuliform type cloudiness.

Figures 5a and b LOW3 images show distinct temporal changes in the maritime air mass from scattered low-level stratiform cloudiness (larger droplets per unit volume) in the morning, to a uniform areal cloud coverage consisting of more droplets per unit volume with smaller droplet sizes by the afternoon. The continental air mass shows similar areal development of lower clouds throughout the day (scattered

clouds in the morning increasing to broken areal coverage by afternoon).

c. Cross-section Results

(1) Optical Depth (TTHG)

Figures 6, 7, 9, and 10 show clearly that optical depth values increase in a west-to-east direction, with a total change of .08. Figures 8 and 11 depict steady optical depth values associated with the southern track which is on the periphery of the maritime/continental transition region and therefore does not show the characteristic parameter changes across the track.

(2) S12 Values

Highest values of S12 are located in the cloud-free region where measurable aerosols are present. Figures 6 through 11 show a decreasing pattern of S12 values in the cloud-free region going west-to-east (ranging from 2.24 to 1.16 respectively). Normally, when traversing from a maritime to a continental regime, values of S12 are expected to increase (see Chapter II). This decreasing pattern could be due to the fact that maritime air is being advected into the area at the surface such that there is continental air above a surface maritime air mass (Figure 3b). The increase in optical depths seen in Figures 6, 7, 9, and 10 in conjunction with this decrease in S12 values confirms an influx of larger

particles of continental origin from Saharan sources into a smaller continental aerosol regime (Johnson and Taylor, 1992).

(3) LOW1

Figures 6, 7, 9, and 10 show generally higher values of LOW1 in the maritime (.40 to .64) than in the continental air mass (.10 to .40). This pattern indicates an increase in areal cloudiness of the maritime region. Figures 8 and 11 show variable patterns of values across the track. This is due to the track location in the southern periphery of the cloudy region characterized by widely scattered, cellular cloudiness.

(4) LOW3

Figures 6, 7, and 10 show generally decreasing values of LOW3 west-to-east in both the continental and maritime regions, ranging from .30 to .10 and .42 to .23 respectively. The increased LOW3 values can be associated with the influx of continental aerosols into the area. Increased numbers of CCN produce a decrease in the radius of the droplets and therefore an increase in LOW3 values. Figure 8 depicts variable values as the track lies entirely within cloudy regions. Figure 9 shows a generally increasing pattern west-to-east in the maritime region with LOW3 values ranging from .24 to .34. This is due to an area of increased brightness present along Track A in the extreme eastern portion of the region (see Figure 5b). As in the continental

region, increased brightnesses are due to a reduction in droplet sizes on the eastern side of the maritime regime. Figure 9 LOW3 values in the continental air mass, decreasing from west-to-east, range from .30 to .20. This decrease to .2 infers that larger droplets are present on the eastern side of the continental air along this track. (Note: Figures 9 and 10 show spikes in the data at approximately 380 and 500 kilometers (km) respectively. These spikes are due to bad imagery data points and should be disregarded).

2. CSD2 (15 June, 1992)

a. Synoptic Summary

At 500mb (not shown), the vortex west of the Azores drifts eastward and fills as a high center develops north of the Azores near 43N25W. The upper-level ridge axis continues to extend along a line from approximately 50N05W to 30N40W. At the same time, the vortex south of Portugal begins to fill and drift northward. At the surface, a strong 1033mb high pressure center near 50N28W ridges southward along 30W to dominate the weather pattern. A slowly moving cold frontal system lies west of the ridge. The persistent low pressure center over Portugal in combination with the strong ridge continue to maintain a northeasterly flow over the project area (Figure 12).

Figure 13a shows that air parcels over the western and central operating area at the 700mb level are transported

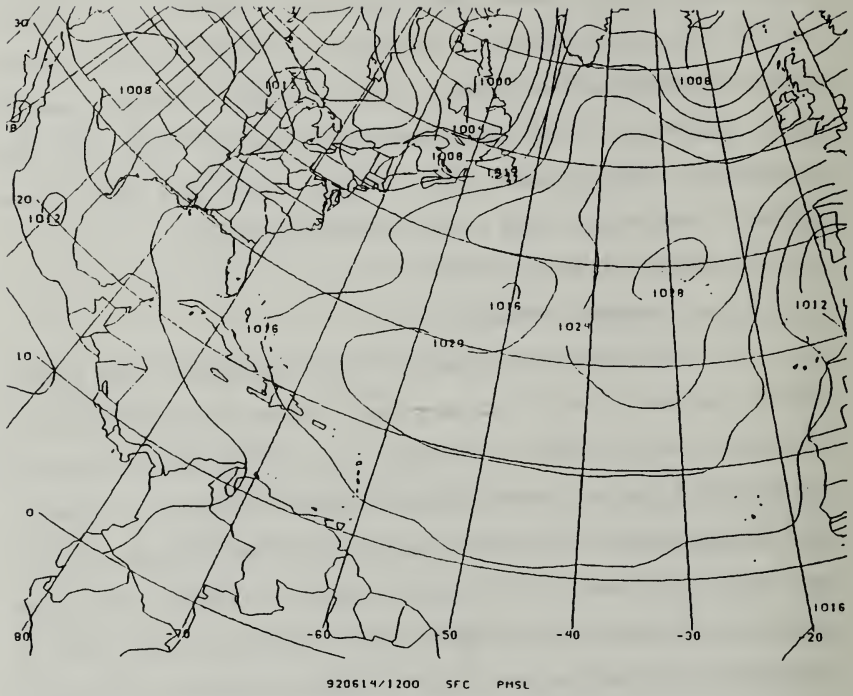

Figure 2. Surface Pressure Chart valid 1200 UTC 14JUN92

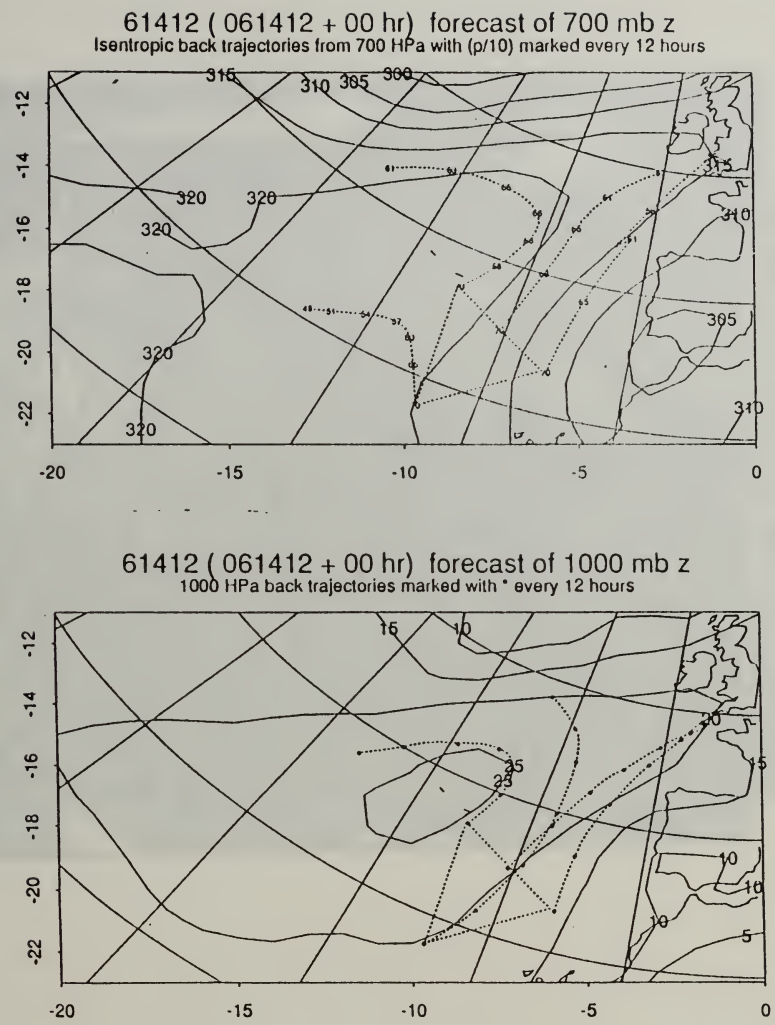

Figure 3. 14JUN92 Back Trajectories Within the Project Region: (a) 700mb and (b) 1000mb

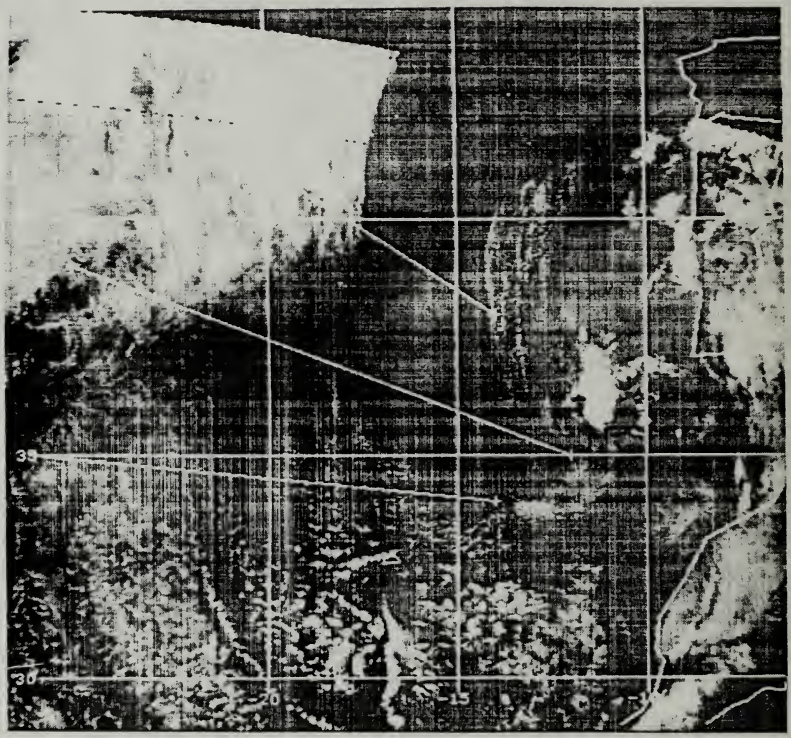

Figure 4a. LOWI Satellite Image at [illegible] 14JUN92

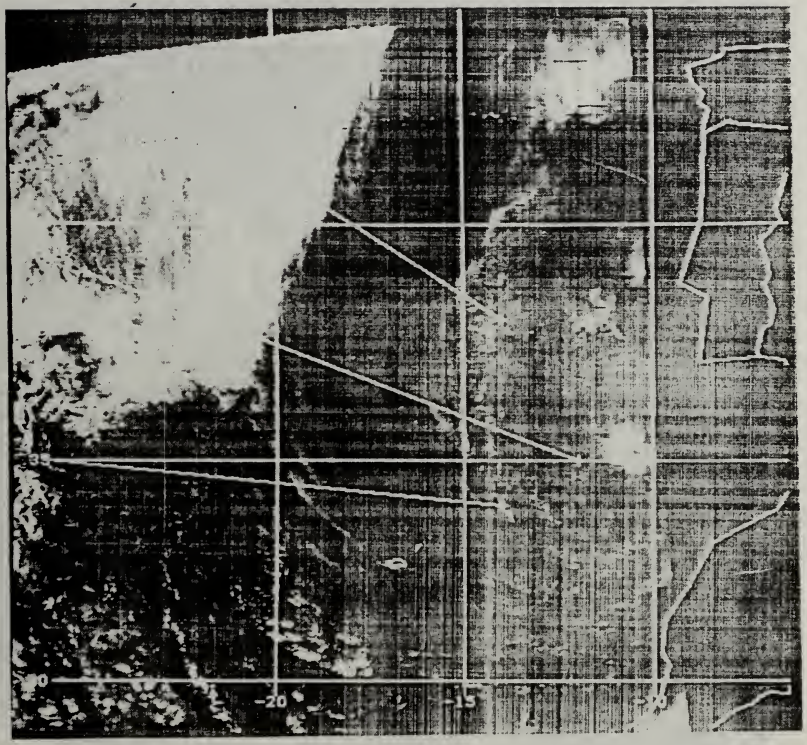

Figure 4b. LOW 1 Satellite Image of [illegible]

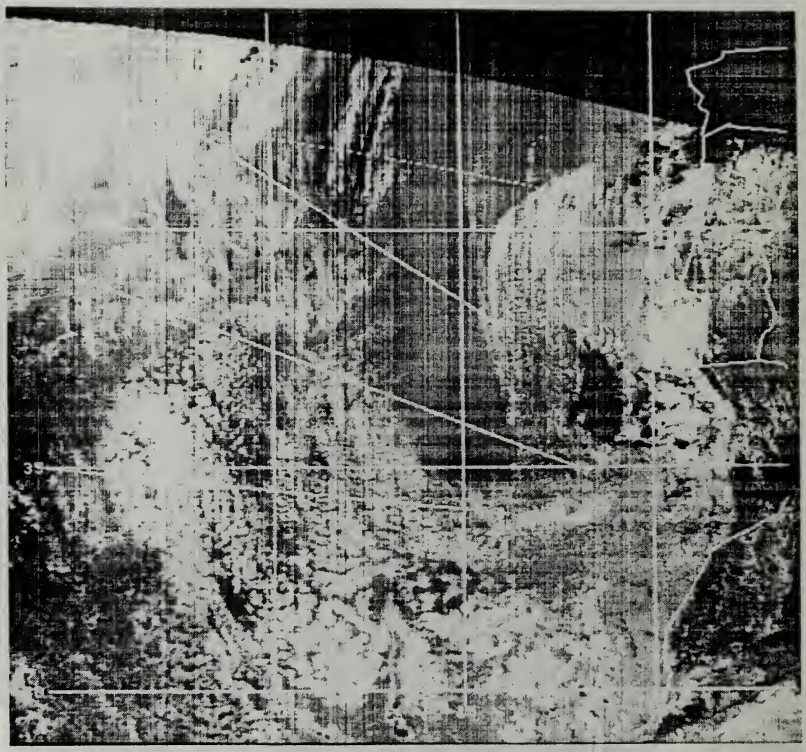

Figure 5a. LOW3 Satellite Image of [illegible] UTC 14JUN82

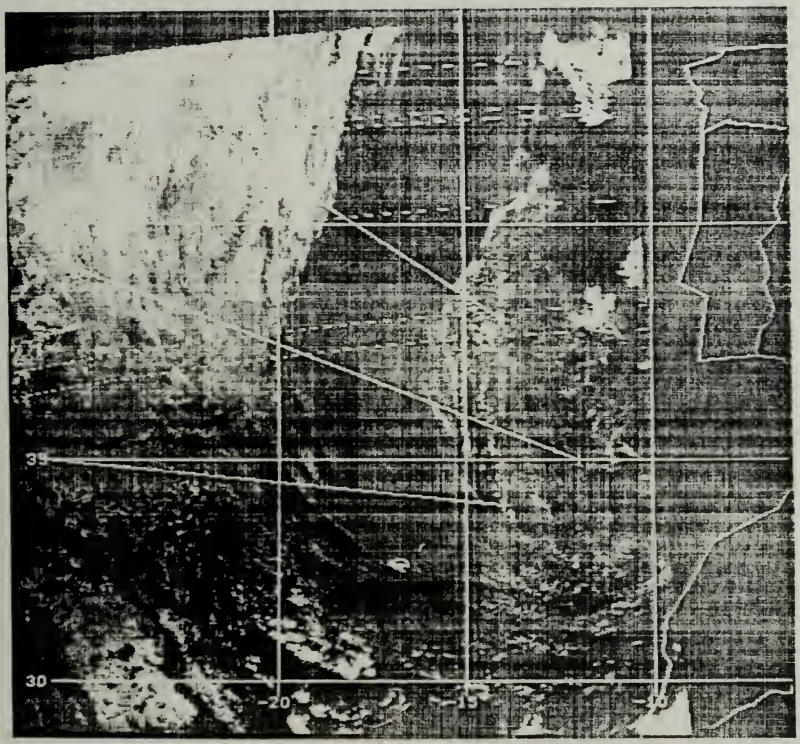

Figure 5b. LOW3 Satellite Image of 162530 UTC 14 JUN 92

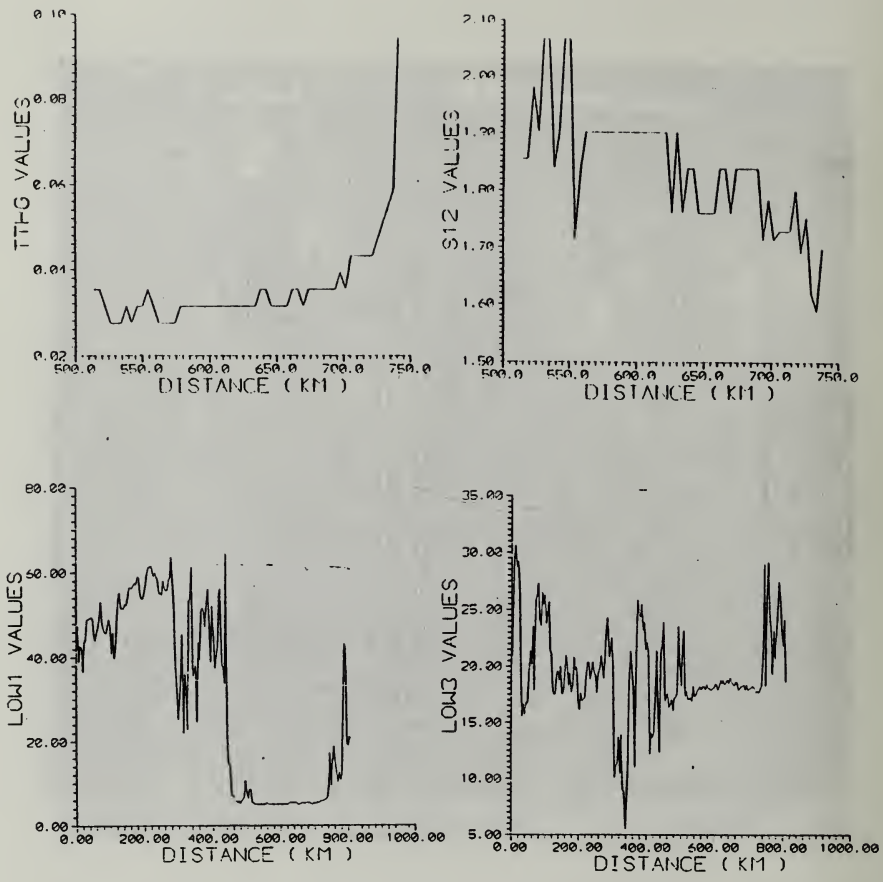

Figure 6. Parameter Results from 090330 UTC 14JUN92: Track A

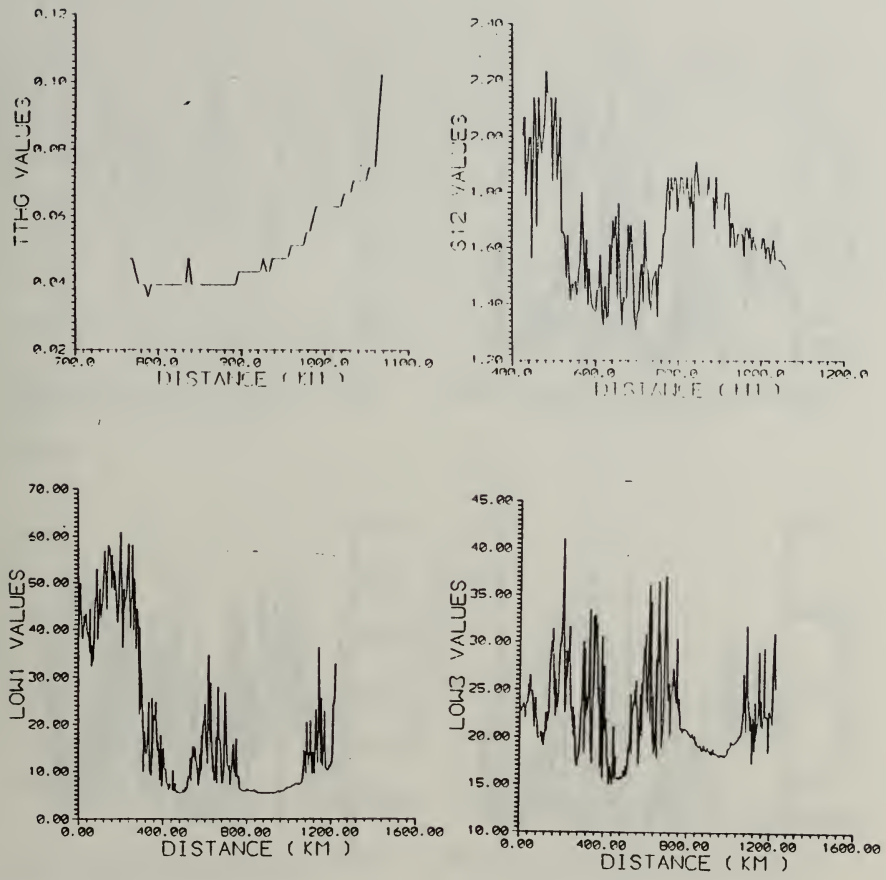

Figure 7. Parameter Results from 090330 UTC 14JUN92: Track B

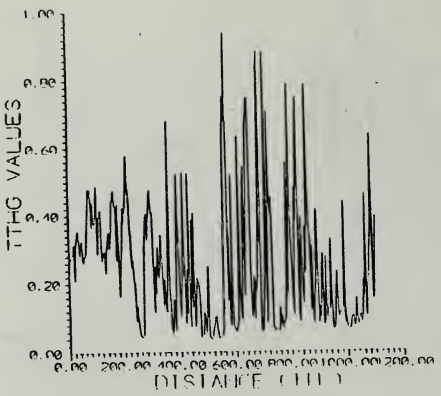

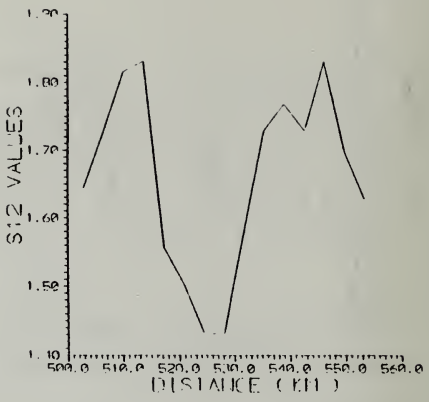

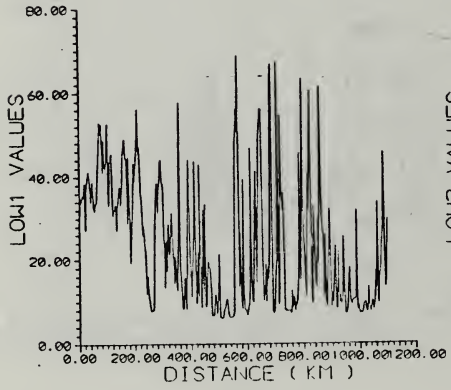

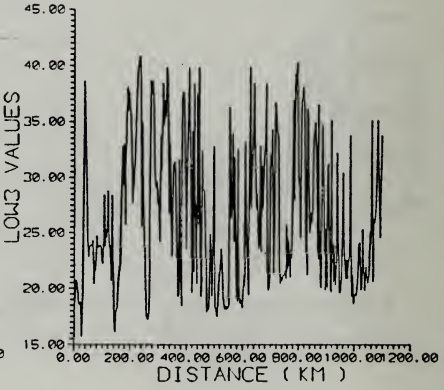

Figure 8. Parameter Results from 090330 UTC 14JUN92: Track C

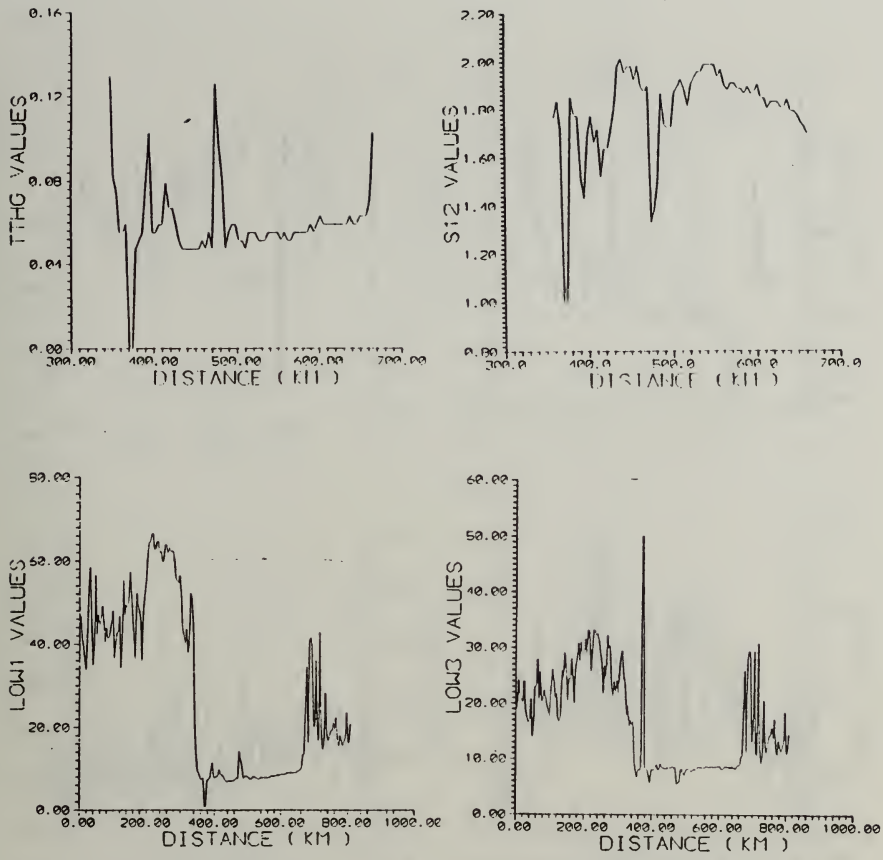

Figure 9. Parameter Results from 162530 UTC 14JUN92: Track A

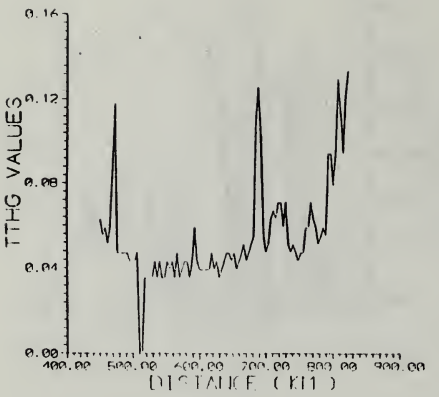

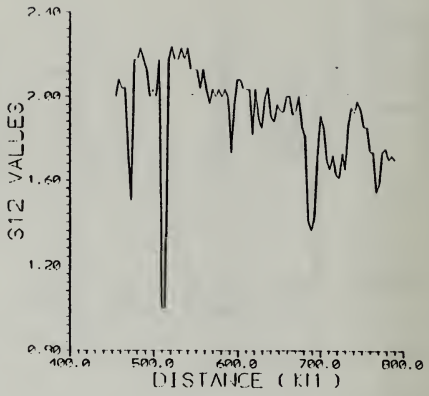

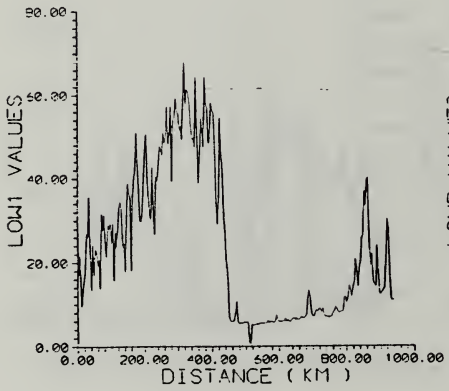

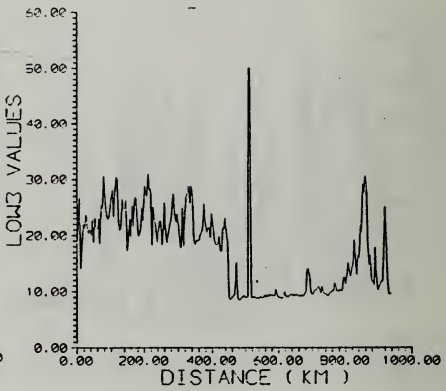

Figure 10. Parameter Results from 162530 UTC 14JUN92: Track B

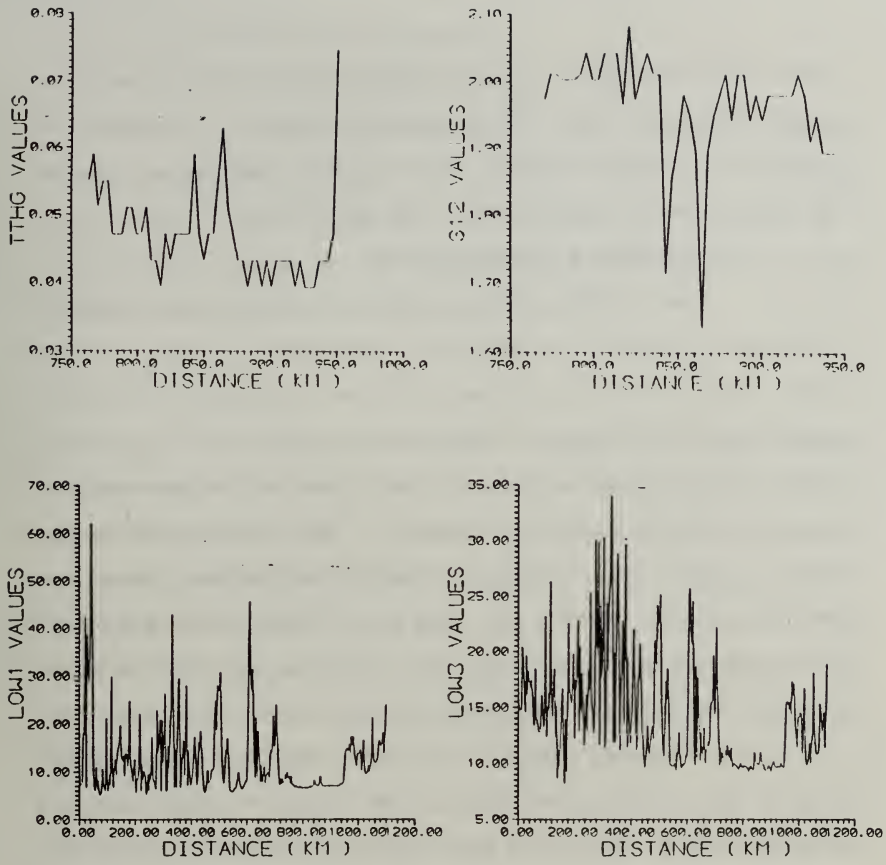

Figure 11. Parameter Results from 162530 UTC 14JUN92: Track C

from a maritime regime, with the eastern portion continuing to originate from the United Kingdom region. Figure 13b indicates that continental air is being advected into the central project region (under the maritime air).

b. Satellite Interpretation

As in CSD1, Figures 14a and b LOW1 images show the continuing presence of brighter cloudiness in the maritime region with an areal distribution of mostly broken to overcast stratocumuliform clouds. The central region shows a distinct swath of cloud-free air being advected around the western side of the surface low over Portugal. The continental region shows significant cloud thickness development from the previous day, with an areal coverage of scattered stratocumulus and cumulus clouds. There is a slight decrease in the overall cloud thickness pattern during the afternoon.

Figures 15a and b LOW3 images give a clear indication of cirrus streaks in the maritime region and the predominance of low-level stratiform cloudiness. The bright reflectances depicted in the continental region indicate a decrease in droplet radii across the area. Figure 15b indicates that the clouds in the maritime region may be decreasing in intensity, while the continental air mass appears to be moving south and west and increasing in both areal cloud coverage and thickness.

c. Cross-section Results

(1) Optical Depth (TTHG)

Figures 16 through 21 show increasing optical depth values west-to-east with a total change of .10 across the track. This continues to indicate the pattern of a continental regime on the eastern side, and a maritime regime on the western side of the project area.

(2) S12

Figures 16 through 21 show S12 values peaking in the center of the cloud-free area and tapering off in magnitude to the east and west. All figures show a general decreasing pattern of S12 values west-to-east ranging from 2.3 to 1.7 respectively. This again is due to the mixture of the continental and maritime air masses (Figures 13a and b) with continental aerosols entering from the northeast, consisting of larger dust particles of Saharan origin (Johnson and Taylor, 1992). (Note: S12 values of 1.00 in figure 16 are in regions of bad satellite data points and should be disregarded).

(3) LOW1

Figures 16 and 17 show comparible values of 20 to 60 in both continental and maritime regions (when the clouds are thicker). Figure 18, at the southern periphery of the cloud activity, shows more variability. Figures 19 and 20

show a general decrease in LOW1 values in the continental regime, correlating with the shift of the cloud patterns and decreased thicknesses of the associated clouds by the afternoon. The peak values in LOW1 seen in Figure 21 in the eastern extreme of the continental air mass correlates with enhanced cloud activity in this area (as seen on Figure 14b).

(4) LOW3

Figures 16 through 19 show slightly higher LOW3 values associated with the maritime western region than during CSD1. This would indicate that there is a greater number of aerosol particles in this region than in the continental region resulting in smaller droplets and increased LOW3 values. As the continental air is advected into the region from the northeast and into the eastern and central portions of the project area (see Figures 13a and b), the associated industrial aerosols (from western Europe) are injected into the region. This addition of aerosols acts to decrease droplet sizes and therefore increase LOW3 values in the continental regime as seen in Figures 20 and 21.

3. CSD3 (16 June, 1992)

a. Synoptic Summary

At 500mb (not shown), a weak trough south of the Azores fills as the ridge extending along 30W continues to build. The vortex over the Iberian Peninsula continues to fill and drift eastward. At the surface, a high pressure

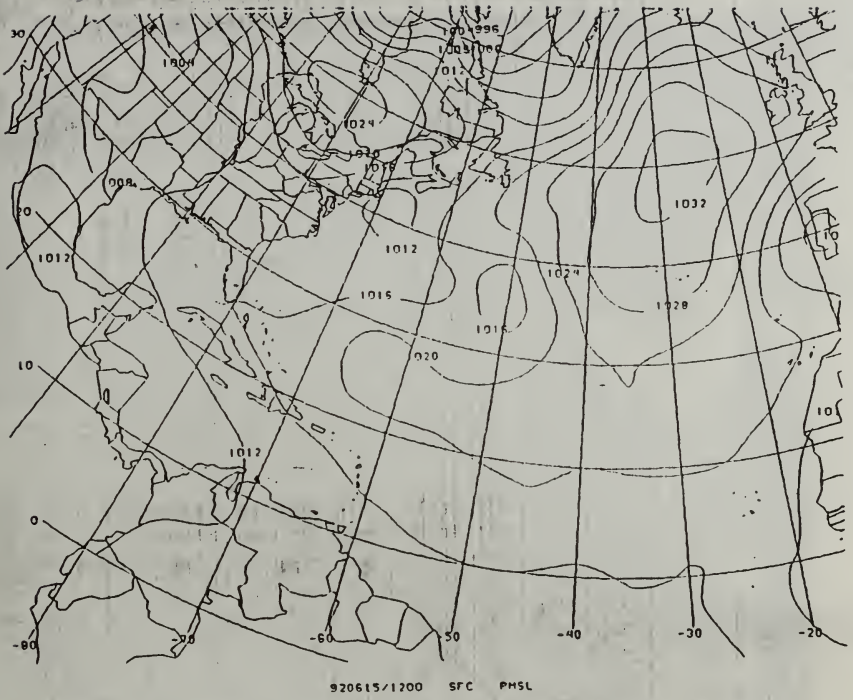

Figure 12. Surface Pressure Chart Valid 1200 UTC 15JUN92

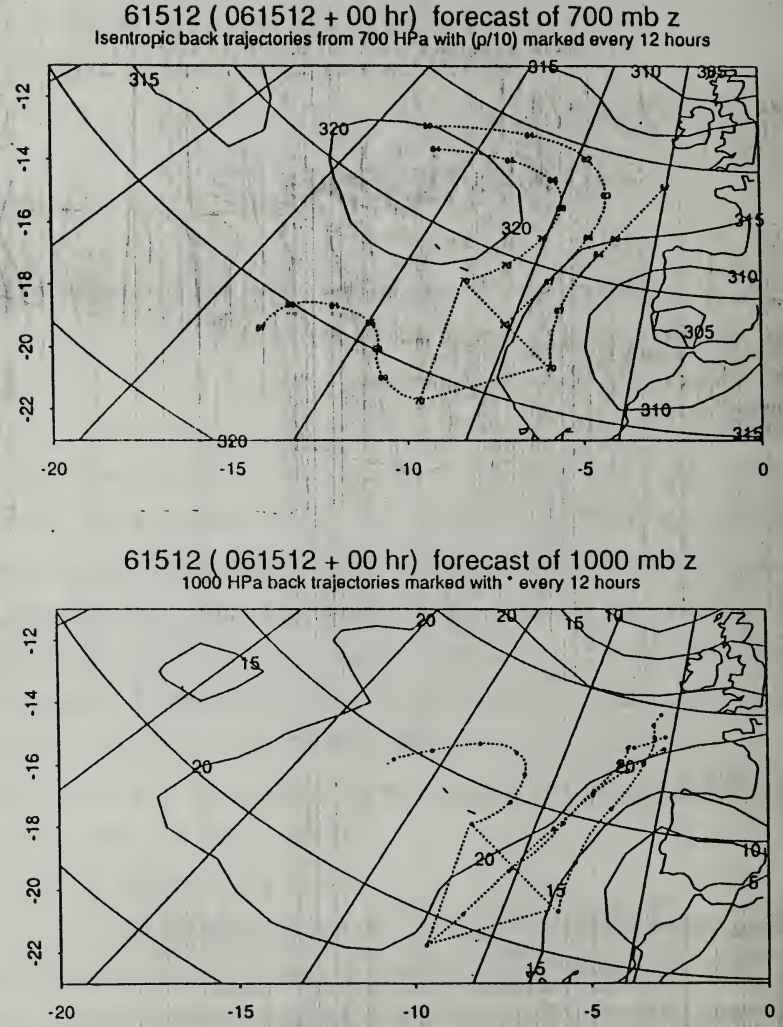

Figure 13. 15JUN92 Back-Trajectories Within the Project Region: (a) 700mb and (b) 1000mb

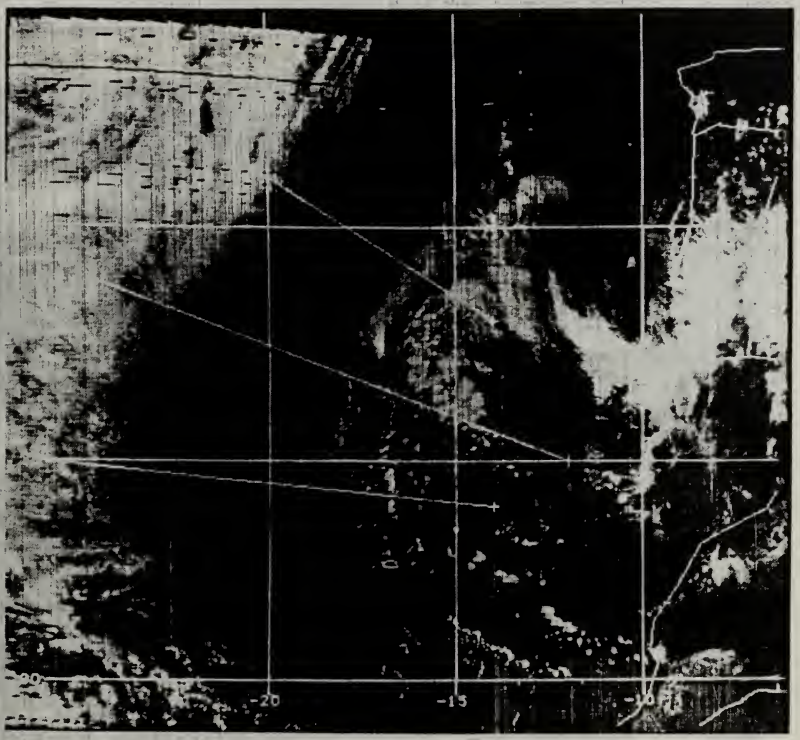

Figure 14a. LOW1 Satellite Image of 084200 UTC 15JUN92

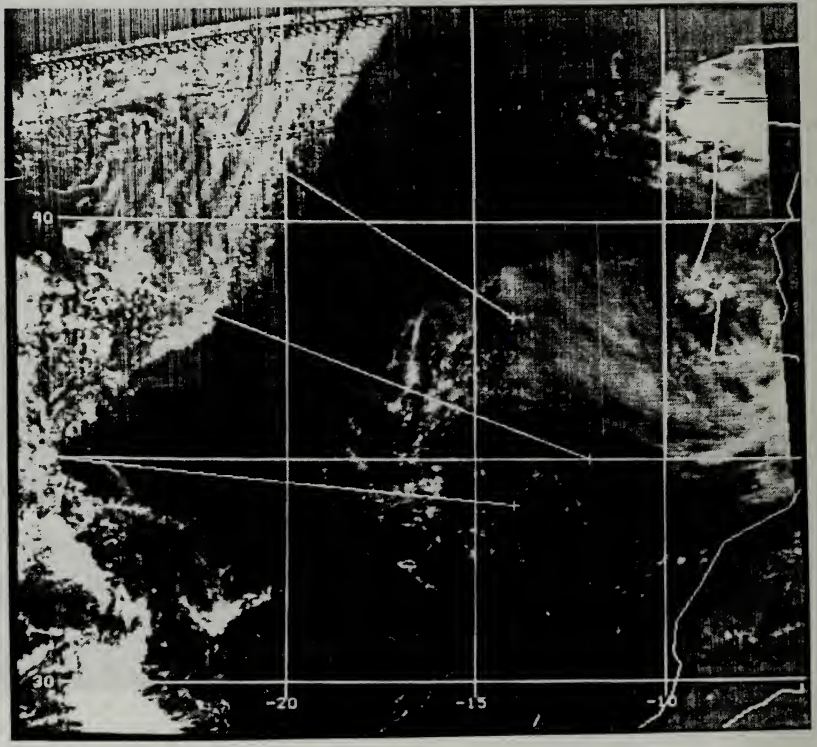

Figure 14b. LOW1 Satellite Image from 161330 UTC 15JUN92

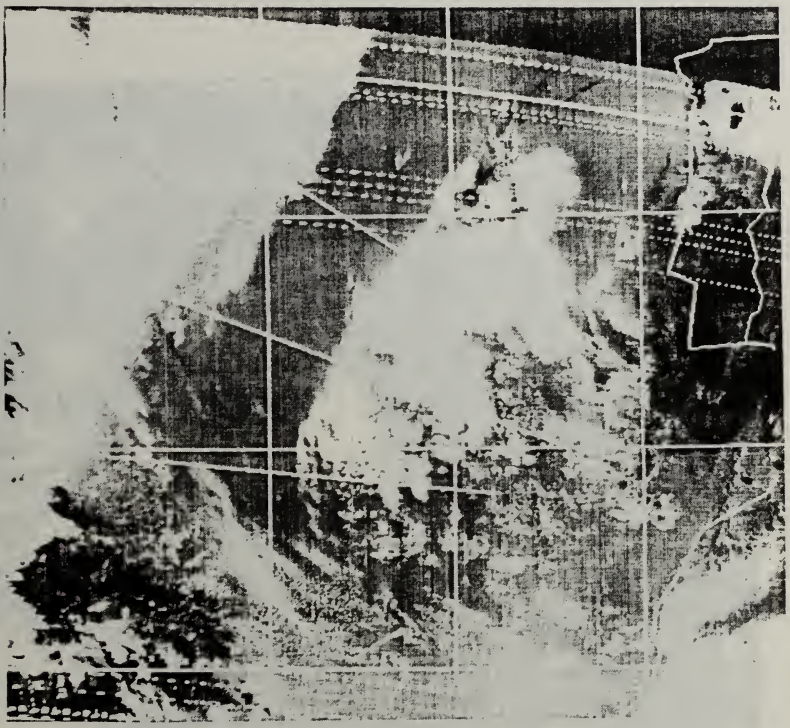

Figure 15a. LOW3 Satellite Image from [illegible] UTC 15JUN92

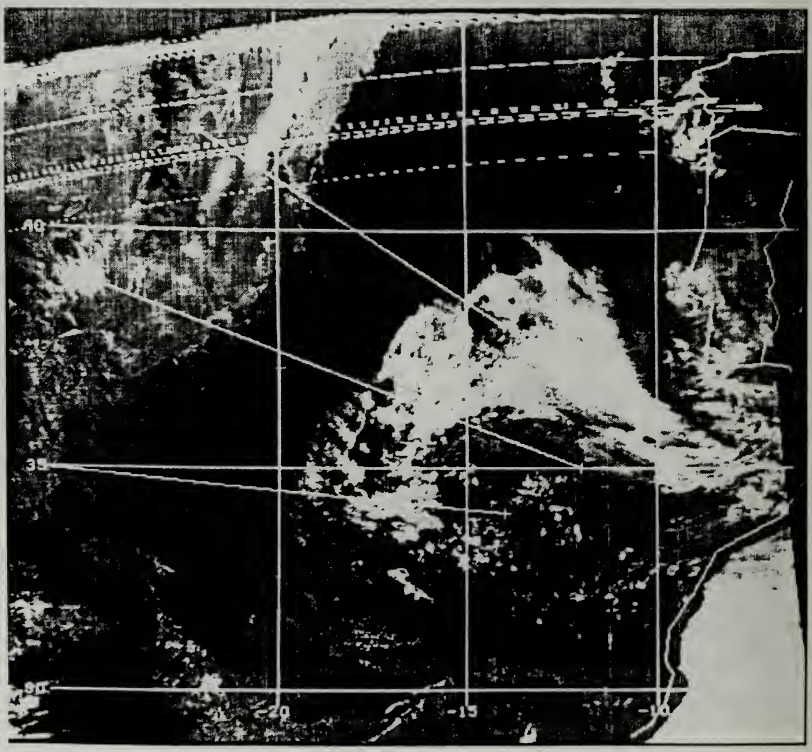

Figure 15b. LOW3 Satellite Image from 161330 UTC 15JUN92

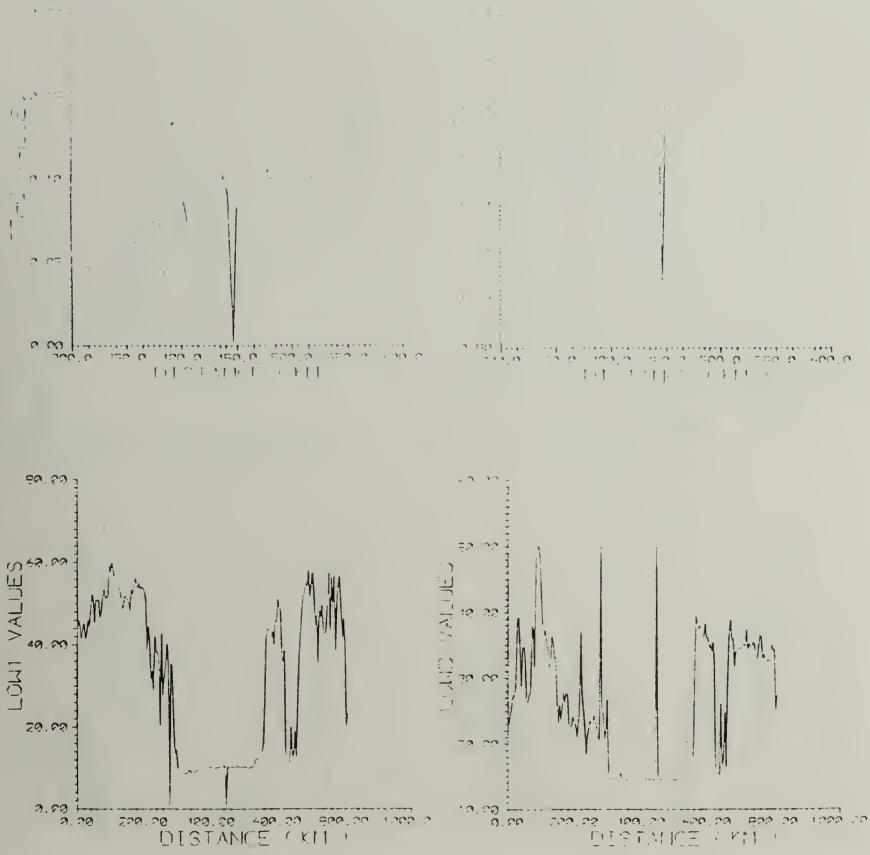

Figure 16. Parameter Results from 084200 UTC 15JUN92: Track A

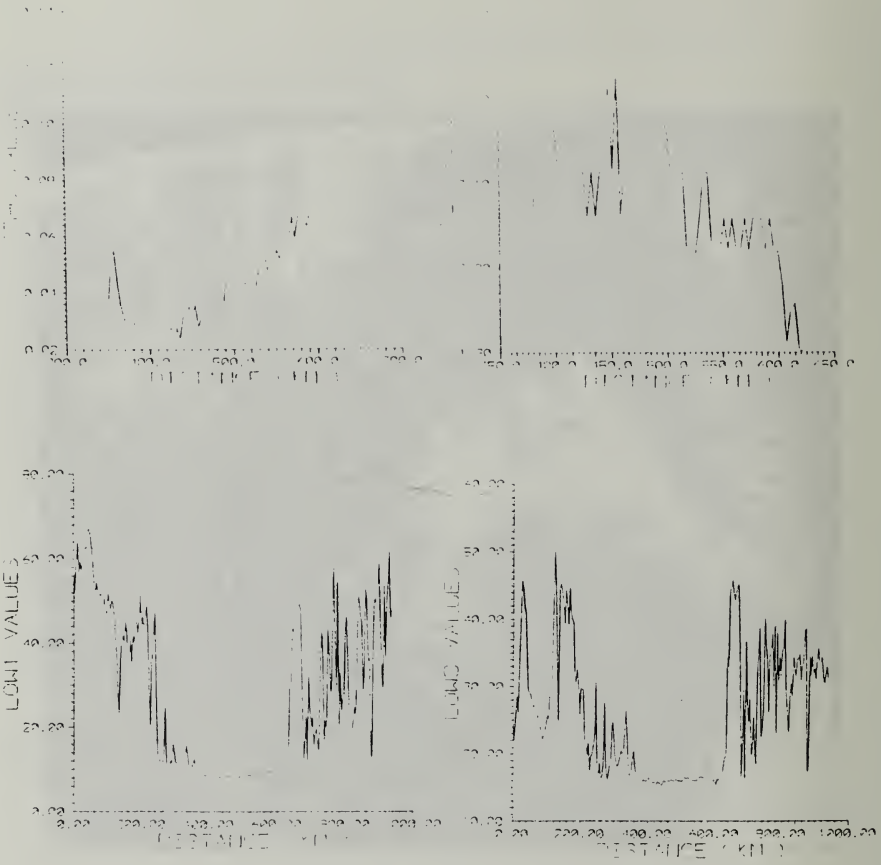

Figure 17. Parameter Results from 084200 UTC 15JUN92: Track B

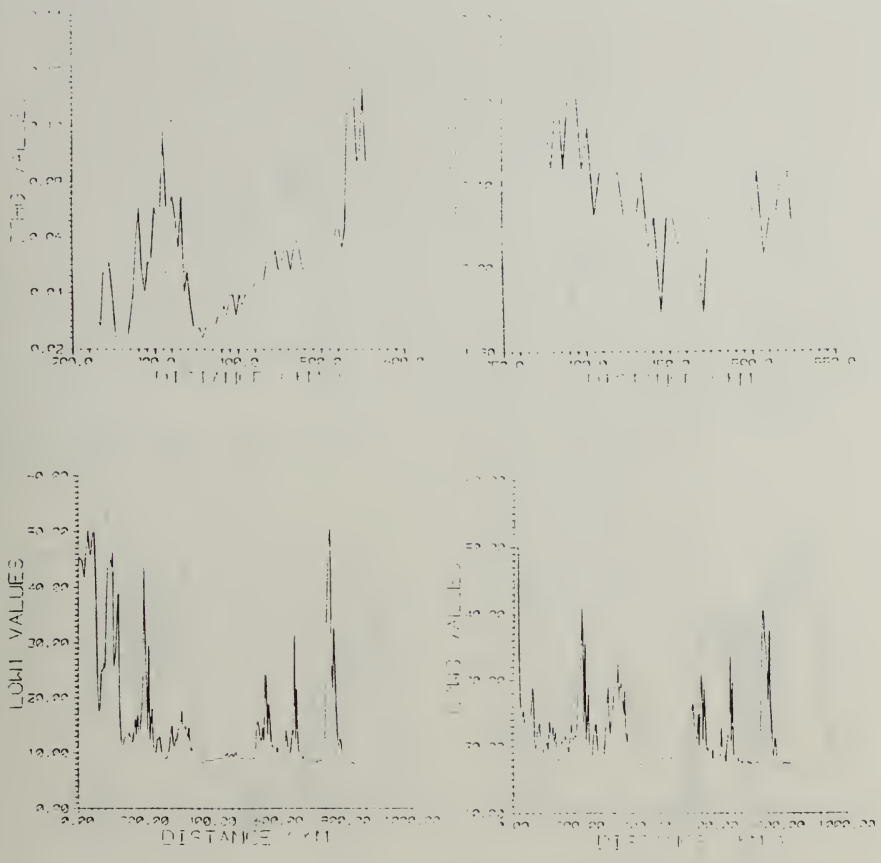

Figure 18. Parameter Results from 084200 UTC 15JUN92: Track C

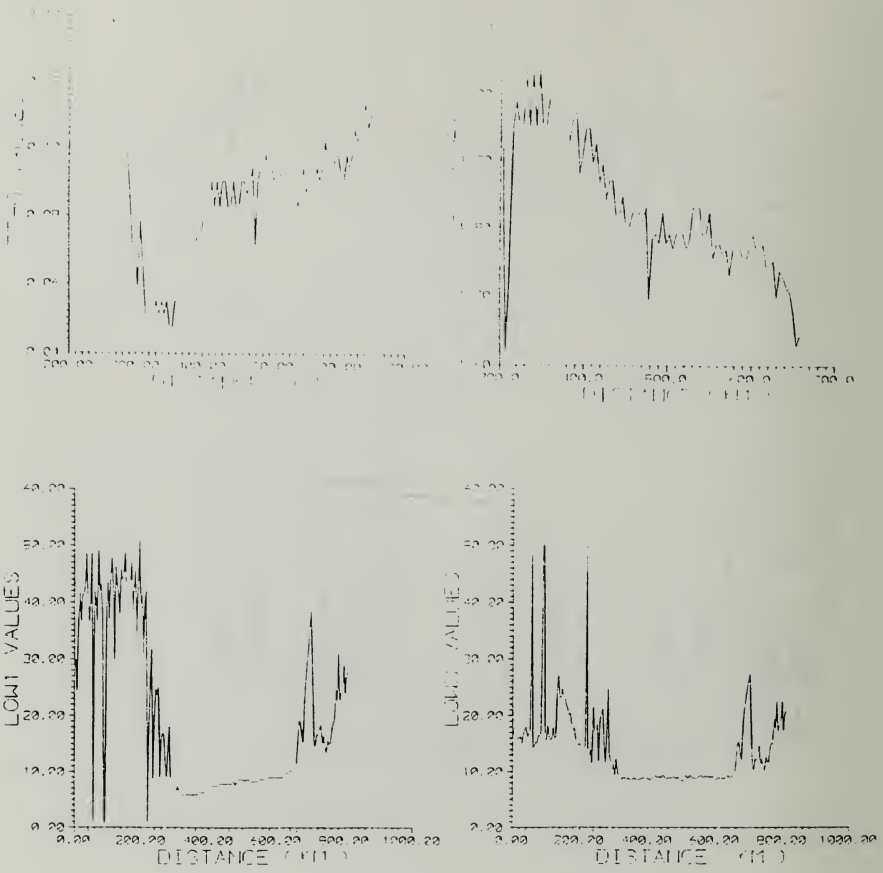

Figure 19. Parameter Results from 161330 UTC 15JUN92: Track A

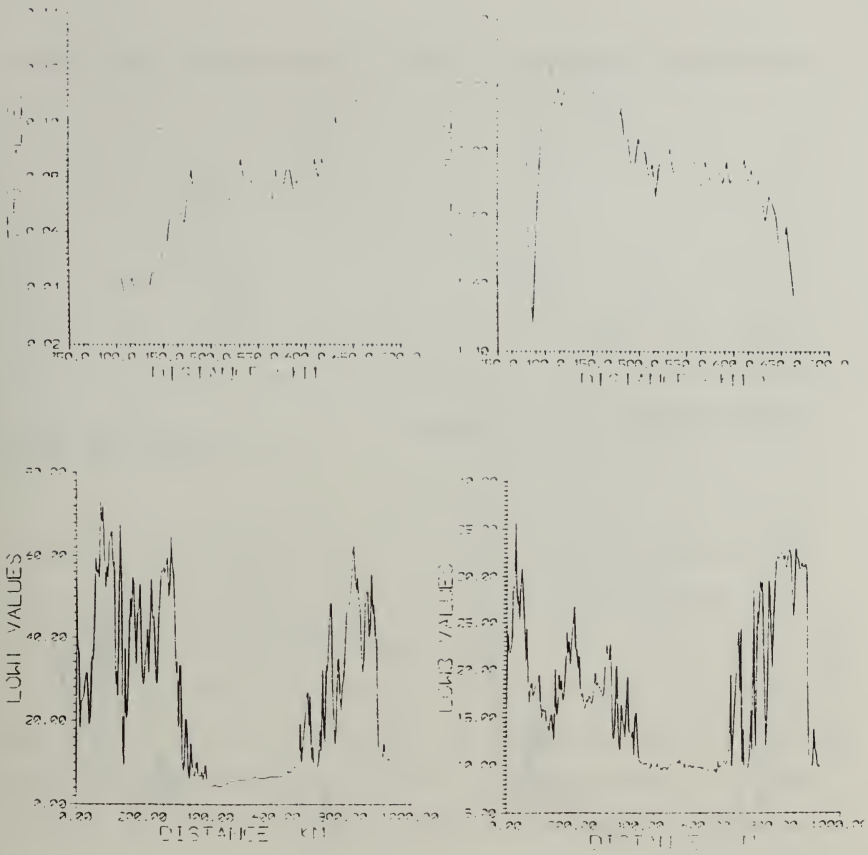

Figure 20. Parameter Results from 161730 UTC 15JUN92: Track B

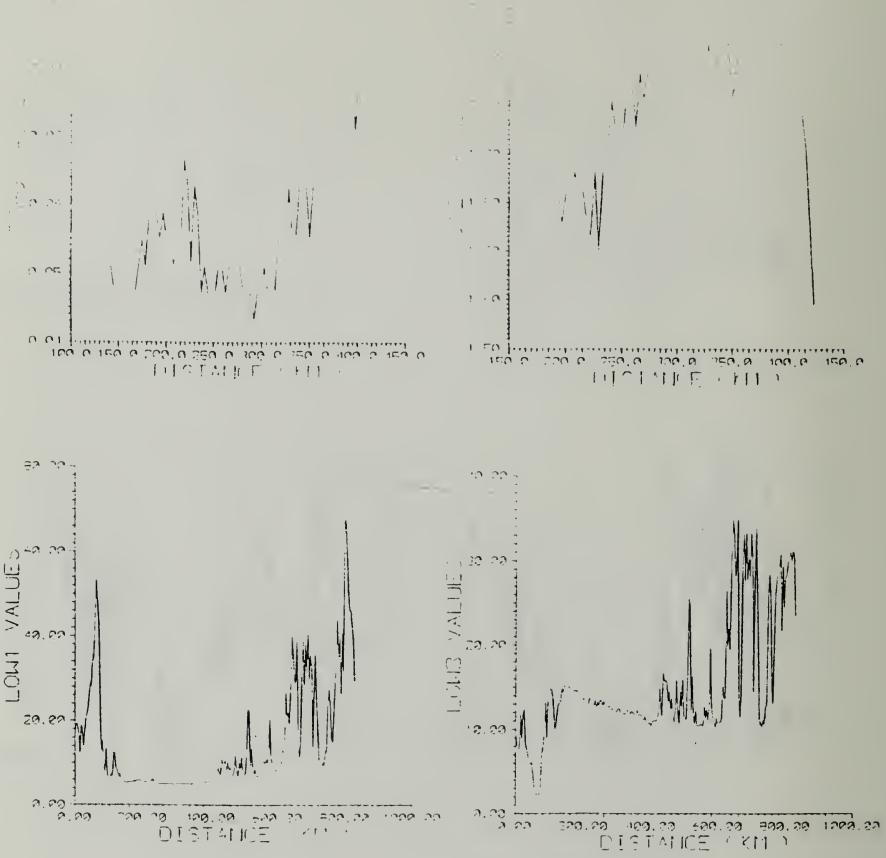

Figure 21. Parameter Results from 161330 UTC 15JUN92: Track C

center near 50N25W builds to 1038mb in response to the upper-level ridge. The ridge will extend northeast-southwest along a line from 60N05E to 40N40W. The low pressure center over central Spain continues to fill and drift eastward. The ridge, in combination with the weakening low pressure system over Spain continue to bring a northeasterly flow to the project area (Figure 22). Figures 23a and b show that parcels over the western operating area continue to be of maritime origin, while parcels in the central and eastern regions originate from the Iberian Peninsula at 700mb, and just south of Ireland at the surface. The surface pattern suggests the possibility of bringing air of maritime characteristics into the central and eastern portions of the operating area.

b. Satellite Interpretation

Figures 24a and b LOW1 images show an overall decrease in areal coverage in the maritime region. Cloud types consist of scattered cumulus and stratocumulus as well as some cellular cloudiness. There is an enhanced region of more reflective cloudiness at the eastern extreme of the maritime region. The central region continues to depict a generally "cloud-free" area (which is decreasing in size as the continental region continues moving westward). The continental air mass, consisting of stratus and stratocumulus clouds, shows increased thicknesses and covers a more extensive area than on previous days. There is also a region

in the southwestern portion of the continental regime that shows convective activity increasing throughout the day.

Figures 25a and b LOW3 images show cloud thickness development in the continental region as well as the presence of low-level cloudiness in the previously cloud-free region. Figure 25a shows a line of more reflective clouds at the extreme eastern edge of the marine air mass. As with the LOW1 reflectances, Figure 25b depicts increased brightness and enlargement of the continental air mass by the afternoon.

c. Cross-section Results

LOW3 imagery (Figures 25a and b) indicates that the previously cloud-free region has developed low-level cloudiness and therefore invalidates optical depth and S12 value studies for this day.

(1) LOW1

Figures 26 and 27 show generally higher LOW1 values in the maritime air mass (.30 to .50) due to the line of enhanced convection (defined by brighter, thicker clouds) in the extreme eastern portion of the region. Figure 27 also shows increased LOW1 values at approximately .53 in the western extreme of the continental air mass in a thicker cloud area. Figure 28 shows increased values in the continental region ranging from .40 to .50 (maritime cloudiness was not sampled within this track). Figure 29 shows highest LOW1 values of .50 to .56 in the continental region, covering more

area than tracks 3 or 4. Figures 14 and 15 depict higher LOW1 values in the continental region and lower values in the more cellular maritime regime.

c. LOW3

Figures 16 and 17 depict lowest LOW3 values in the extreme western maritime low-level cloudiness, increasing dramatically from an initial LOW3 value of .15 to .30 and .34 respectively, due to the line of more reflective clouds as seen in Figure 05a. Figures 26 through 28 show a decreasing LOW3 pattern west-to-east across the central region with a slight increase upon entering the continental regime). This decreasing pattern supports the mixing of the cloud masses and the presence of smaller, more numerous droplets in the western part of the continental air mass.

Figures 29 and 30 show increased LOW3 values west-to-east. This is consistent with thickening of clouds in the southwest portion of the continental regime. These LOW3 values also support the weakening of the brighter line of clouds in the eastern extreme of the maritime regime. (Note: The peak values of 50 in figures 29 and 30 are bad satellite data points and should be disregarded). Figure 31 shows low values in less cloudy regions (at 200 to 400 km) and depicts highest values in the continental and maritime air masses as the track traverses thicker, brighter cloudiness. This track is on the southern extreme of the continental and maritime

cloudiness and does not appear to be as influenced by the air mass mixing taking place in the region to the north.

4. CSD4 (17 June, 1992)

a. Synoptic Summary

At 500mb (not shown), a strong ridge axis remains the dominant feature, extending along 25W, with a weak shortwave approaches from the west. The filling vortex over the Iberian Peninsula elongates to the northwest in response to a weak shortwave transitting along the eastern portion of the ridge. At the surface, the high pressure center near 52N25W builds to 1041mb. A ridge axis extends along 28W (south of the high center), and northeast across northern United Kingdom (north of the high center). The ridge axis maintains a northeasterly flow west of Portugal, and an easterly flow west of northern Africa (Figure 32). Figures 33a and b show that parcels at the surface and 700mb over the western operating area continue to be of maritime origin, while parcels over the central and eastern operating area originate from the Bay of Biscay/western Iberia region.

b. Satellite Interpretation

Figures 34a and b LOW1 images show the intrusion of the continental air mass into the maritime regime, with the remnants of the cloud-free region extending in an arc across the center of the image. The cloud-free region is more apparent during the afternoon. Maritime air mass areal

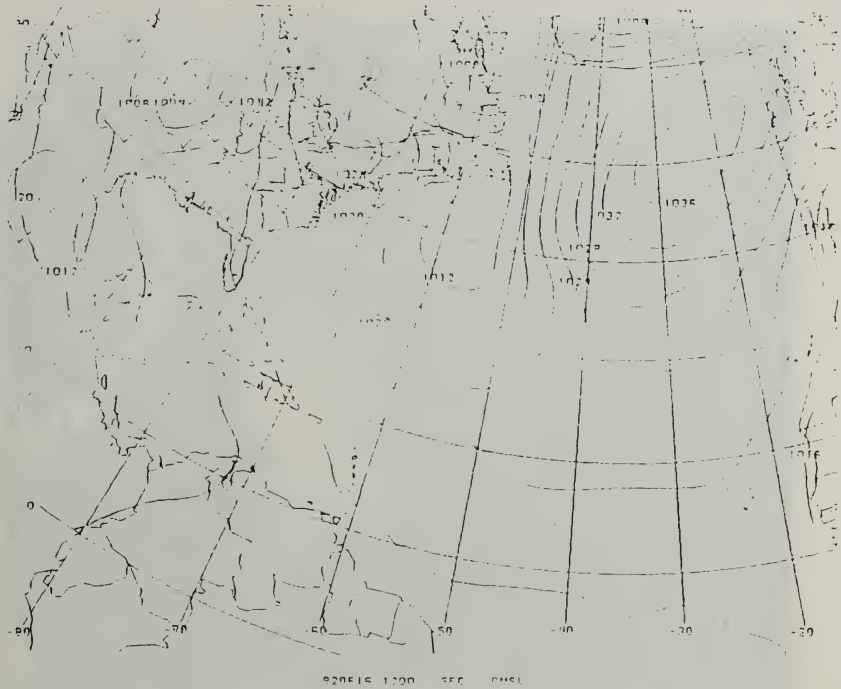

Figure 22. Surface Pressure Chart Valid 1200 UTC 16JUN92

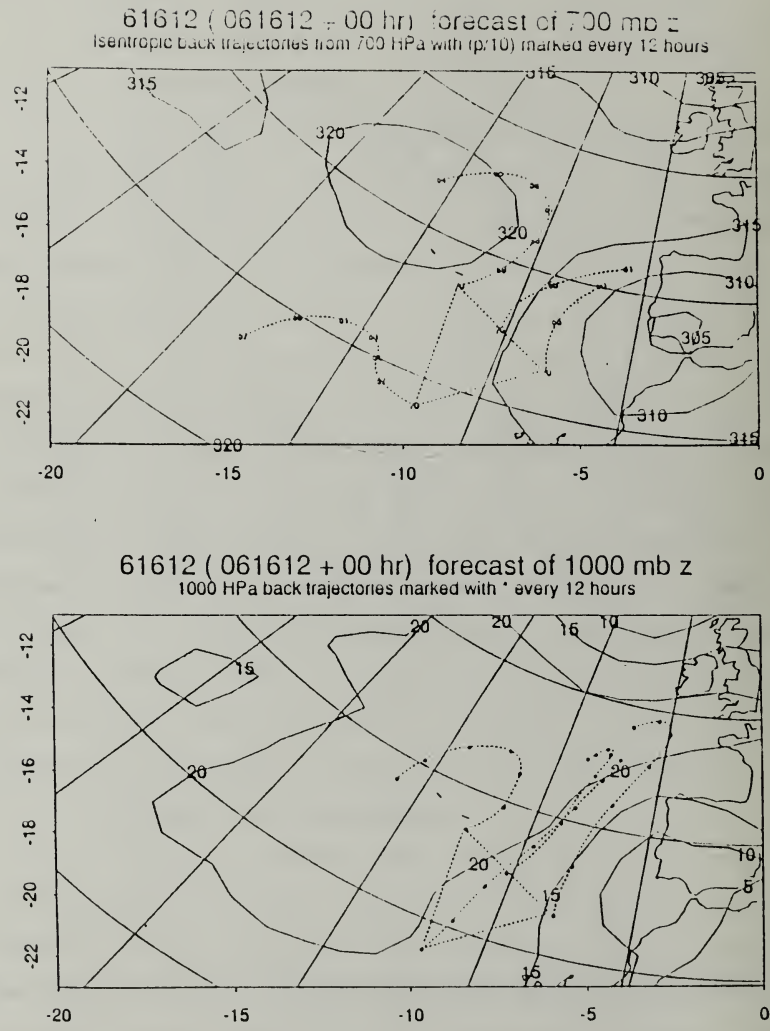

Figure 23. 16JUN92 Back Trajectories Within the Project Region: (a) 700mb and (b) 1000mb

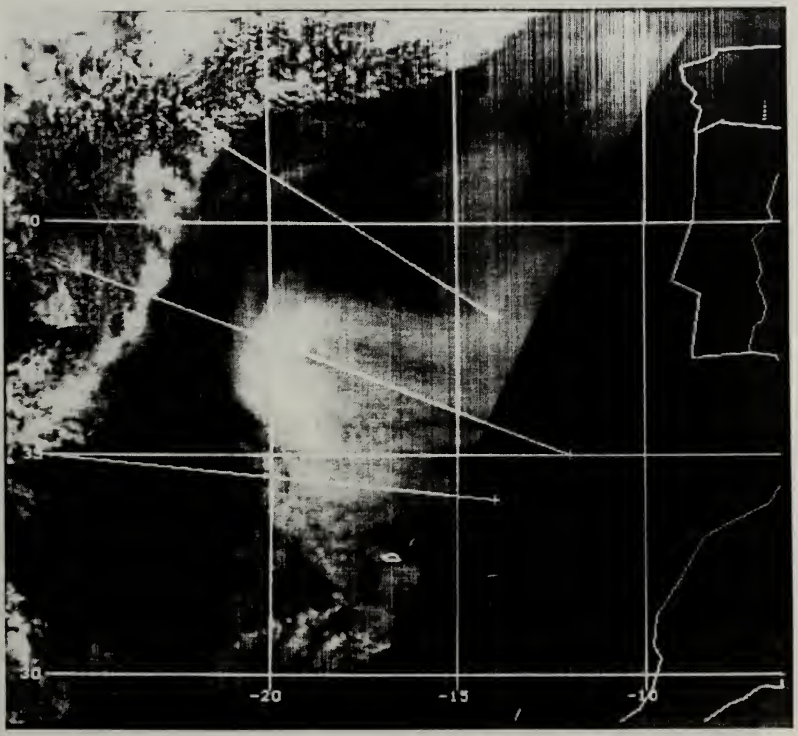

Figure 24a. LOW1 Satellite Image of 095900 UTC 16JUN92

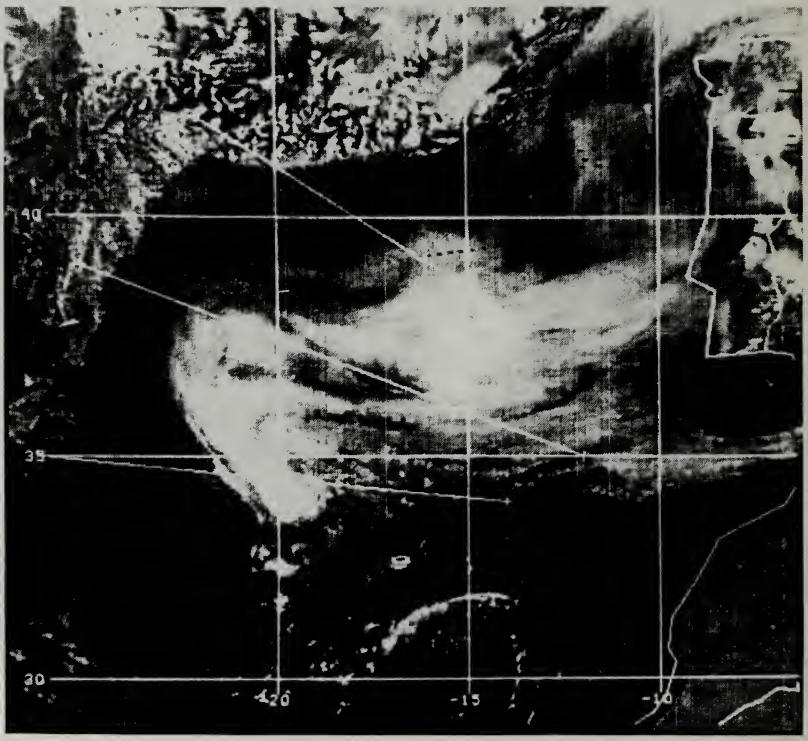

Figure 24b. LOW1 Satellite Image of 160130 UTC 16JUN92

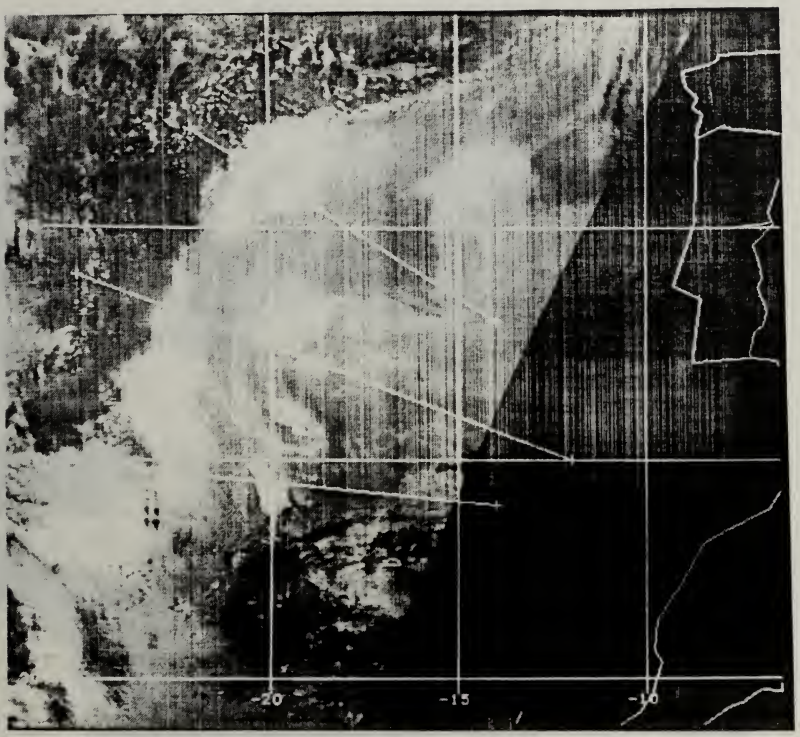

Figure 25a. LOW3 Satellite Image of 095900 UTC 16JUN92

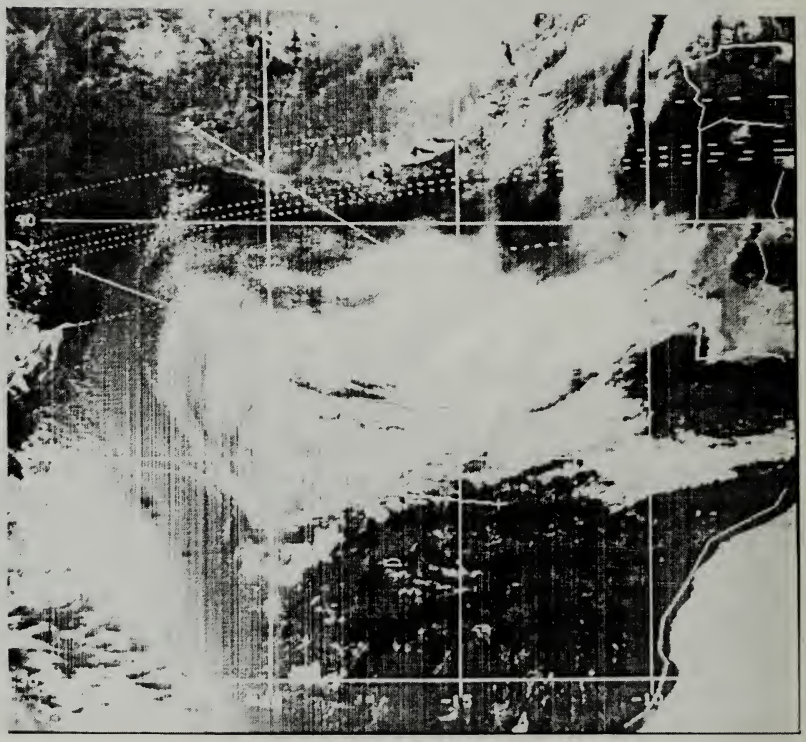

Figure 25b. LOW3 Satellite Image of 160130 UTC 16JUN92

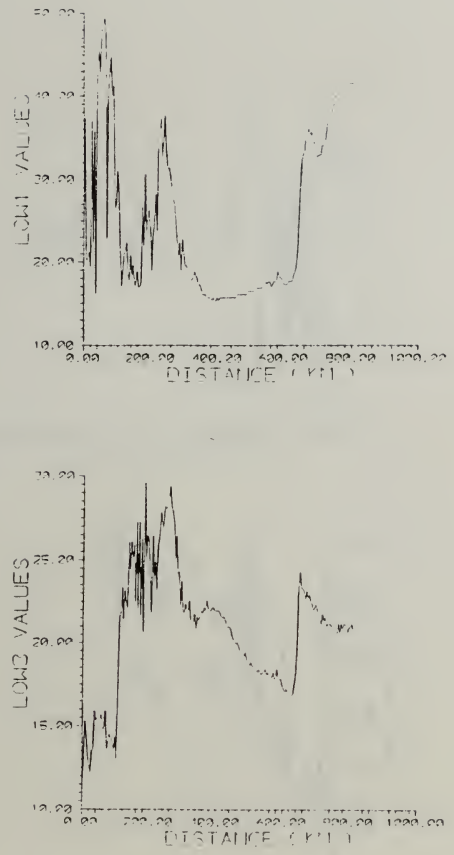

Figure 26. Parameter Results from 095900 UTC 16JUN92: Track A

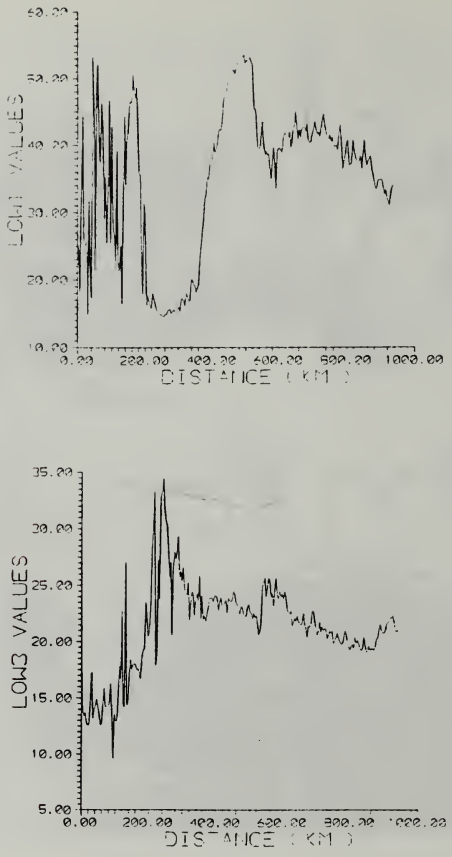

Figure 27. Parameter Results from 095900 UTC 16JUN92: Track B

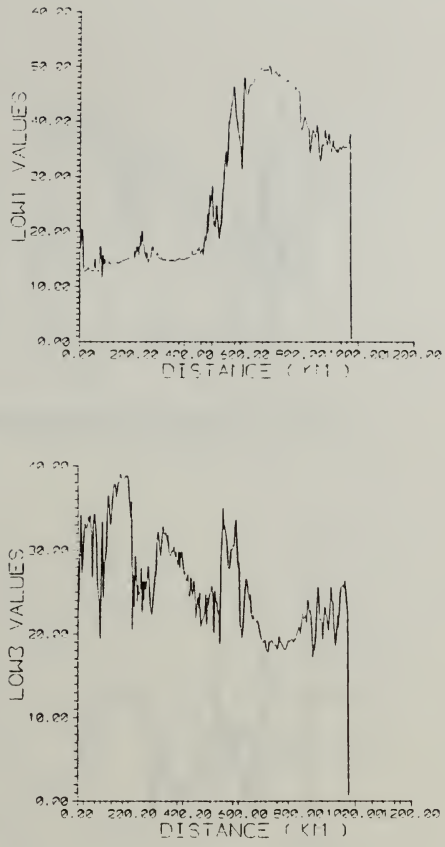

Figure 28. Parameter Results from 095900 UTC 16JUN92: Track C

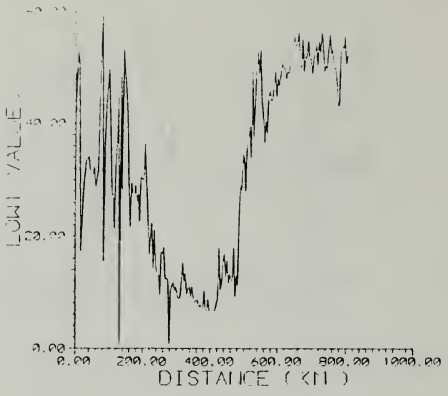

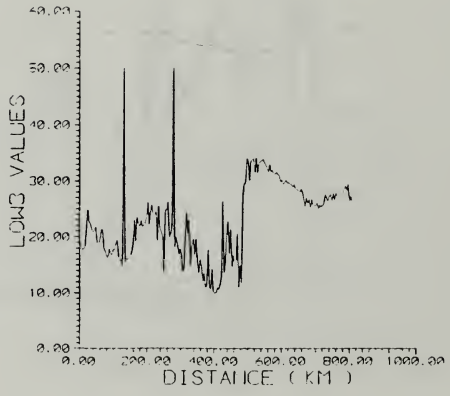

Figure 29. Parameter Results from 160130 UTC 16JUN92: Track A

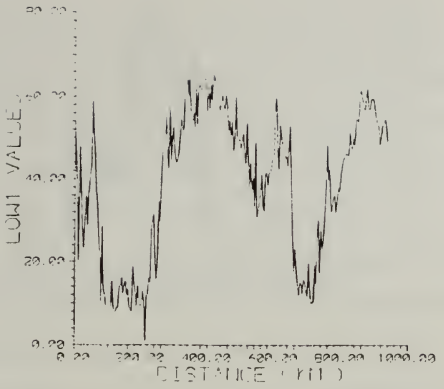

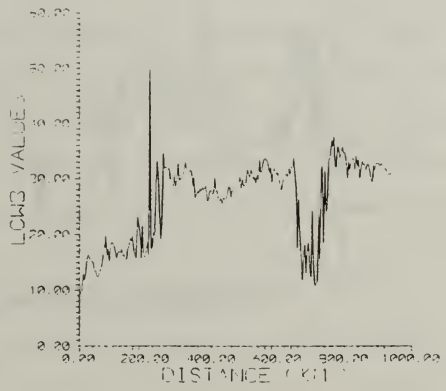

Figure 30. Parameter Results from 160130 UTC 16JUN92: Track B

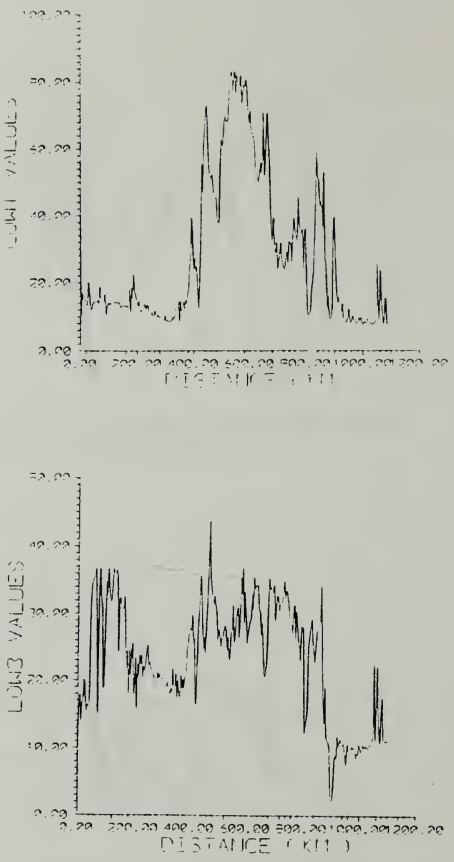

Figure 31. Parameter Results from 160130 UTC 16JUN92: Track C

coverage consists of broken stratocumulus clouds, with stratus and stratocumulus clouds present in the continental air mass (southern and eastern image regions). The continental regime appears more well developed with thicker and brighter reflectances than the maritime.

Figures 35a and b LOW3 images show mostly low-level cloudiness, with more reflective cloudiness present in the eastern extreme of the maritime region. The "cloud-free" region is depicted by areas of thin, low-level clouds or no clouds in the central portion of the image. The continental air mass is characterized by increased cloud reflectances with a cirrus shield present in the southwest portion of the quadrant. The cirrus shield in the southwest portion increases in area by afternoon. A region of uniform cloudiness extends over the eastern portion of the continental air mass.

c. Cross-section results

As with 1115, Figures 35a and b LOW3 images do not clearly depict a cloud-free region for optical depth and S12 studies. Therefore, these parameters are not addressed on this day.

(1) LOW1

Figures 36 and 37 show highest values of LOW1 in the maritime air mass (within thicker cellular cloudiness), with a distinct decrease as less cloudy areas in the central

region are traversed. Figures 33 through 37 depict quite variable LOW1 values across the entire region. Figure 41 shows the characteristic drop in LOW1 values in less cloudy regions, with highest values in the eastern side of the continental regime. The LOW1 data supports the fact that there is more reflective cloudiness in the eastern region than the western in the continental air mass, with the opposite being true in the maritime regime.

(2) LOW3

Figures 36 and 37 verify the low-level, less reflective cloudiness in the maritime air mass region, with the lowest values on the west side (ranging from approximately 15 to 20). LOW3 values increase dramatically west-to-east as the tracks pass into aerosol-rich, more reflective cloud regions. Figure 38 shows highly variable LOW3 values as the track is entirely within the continental region of broken cloudiness. Figure 39 LOW3 values are variable across most of the region, with a decrease on the eastern side in an area of widely scattered low-level cloudiness. Figures 40 and 41 show increasing LOW3 values west-to-east (from .11 to .40 and .2 to .43 respectively) across the entire region. A decrease in droplet size, higher aerosol concentrations, and a shift towards a smaller mean cloud drop radius in the eastern portions of the continental regime due to the influx of aerosols (Saharan dust/European industrial pollutants) account

(9% increased LCL frequency in this region (Mineart, 1988). A comparison of Figures 39a and 39b will show that the overall LCWS Track 1 pattern supports the western movement of the continental air mass in the southern region, while maintaining the east-west separation of continental/maritime characteristics to the north.

5. CSD5 (18 June, 1992)

a. Synoptic Summary

At 500mb (not shown), the dominant ridge feature extending along 30W continues to build to the north as a vortex develops just north of the Azores. The associated shortwave is moving eastward, extending south of the Azores along 30W by 1200 UTC. This shortwave pushes the southern portion of the persistent ridge to the east of the project area. At the surface, the 1041mb high pressure center located near 53N25W ridges north-south along 25W. A developing 1010mb low pressure center located near 40N45W approaches from the west. The persistent low pressure system over central Spain, in combination with the ridge to the west continue to bring a northeasterly flow to the project area (Figure 42). Figure 43a indicates that parcels at 700mb originate over the water in the western and central portions of the project area, while the eastern region parcels originate over the Iberian Peninsula. Figure 43b indicates that at the surface, all parcels in the western and central project area originate from

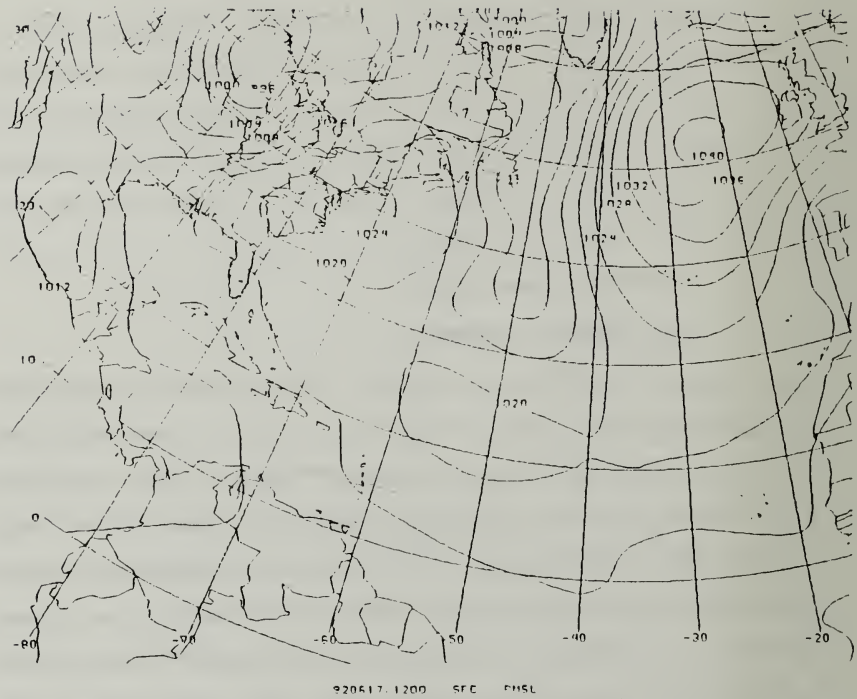
1012
1008
1004
1000
996
1020
1024
1028
1032
1036
1040
1044
1048
1052
1056
1060
1064
1068
1072
1076
1080
1084
1088
1092
1096
1100
1104
1108
1112
1116
1120
1124
1128
1132
1136
1140
1144
1148
1152
1156
1160
1164
1168
1172
1176

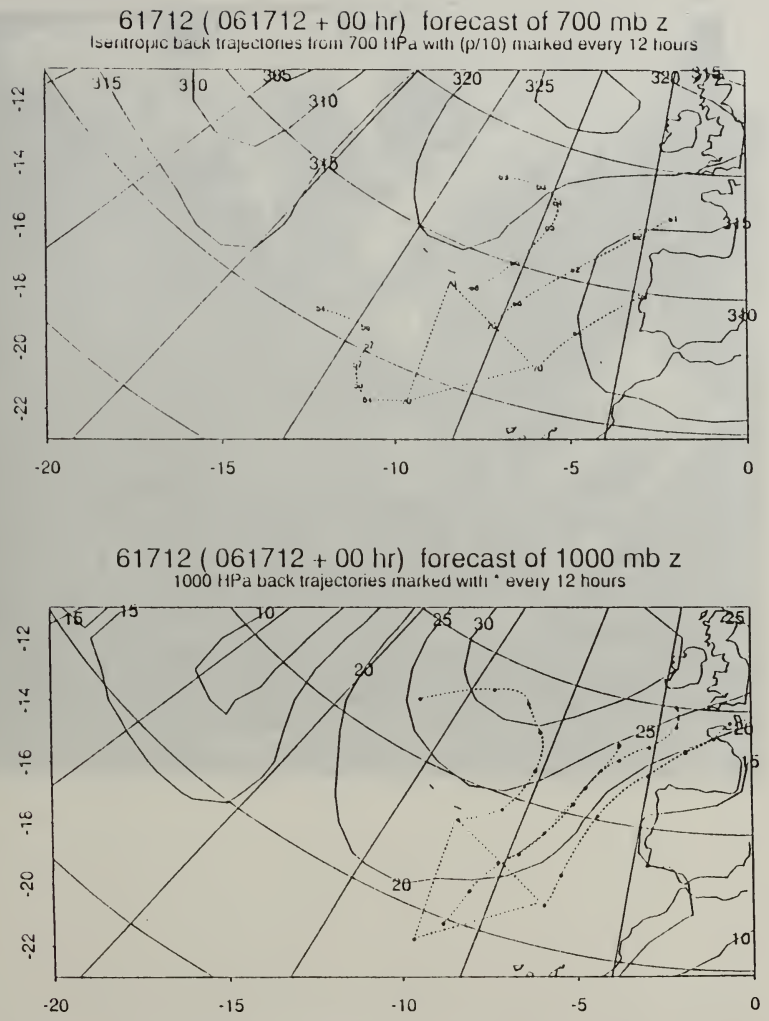

Figure 33. 17JUN92 Back Trajectories Within the Project Region: (a) 700mb and (b) 1000mb

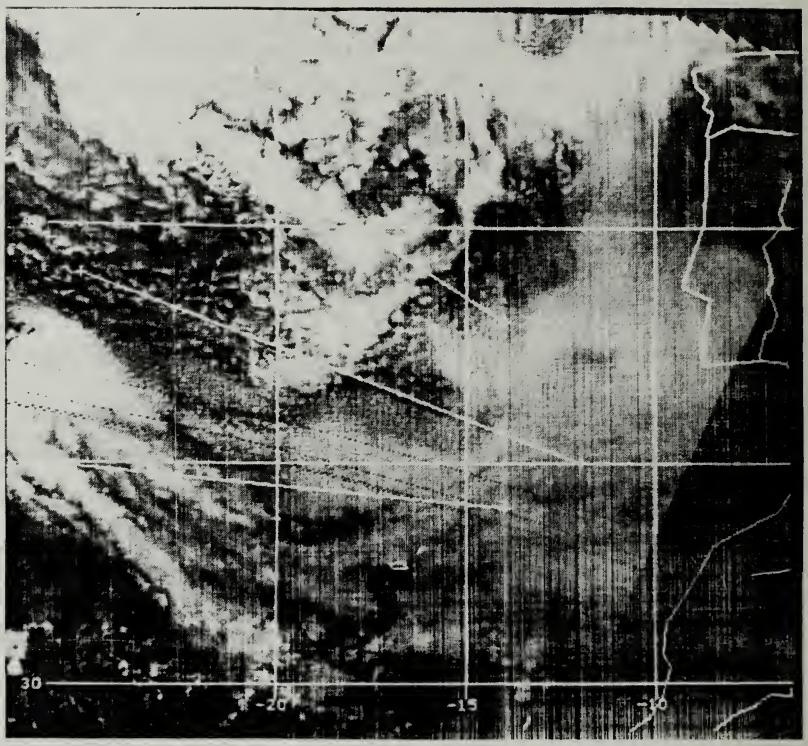

Figure 34a. LOW1 Satellite Image of 093900 UTC 17JUN92

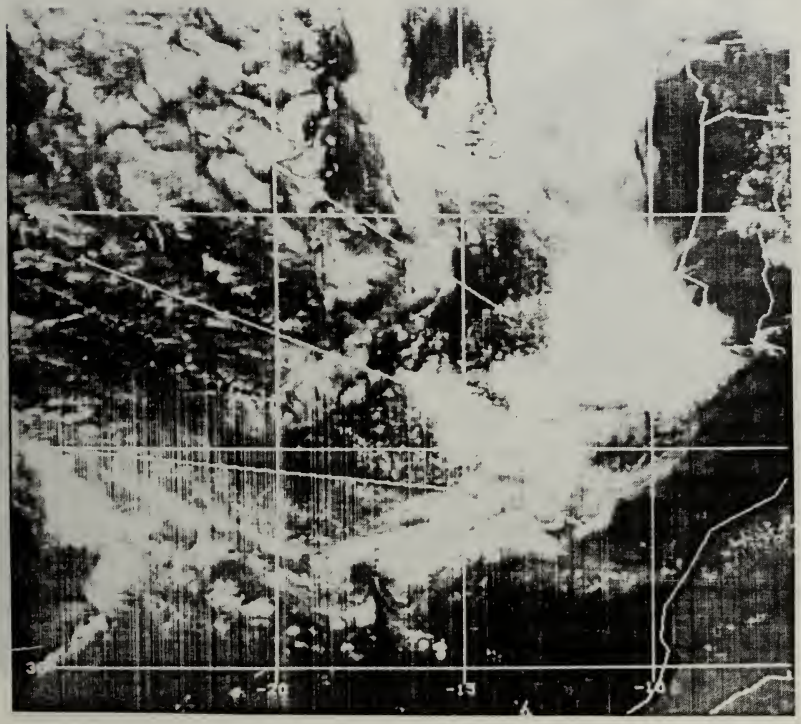

Figure 34b. LOW1 Satellite Image of 154930 UTC 17JUN92

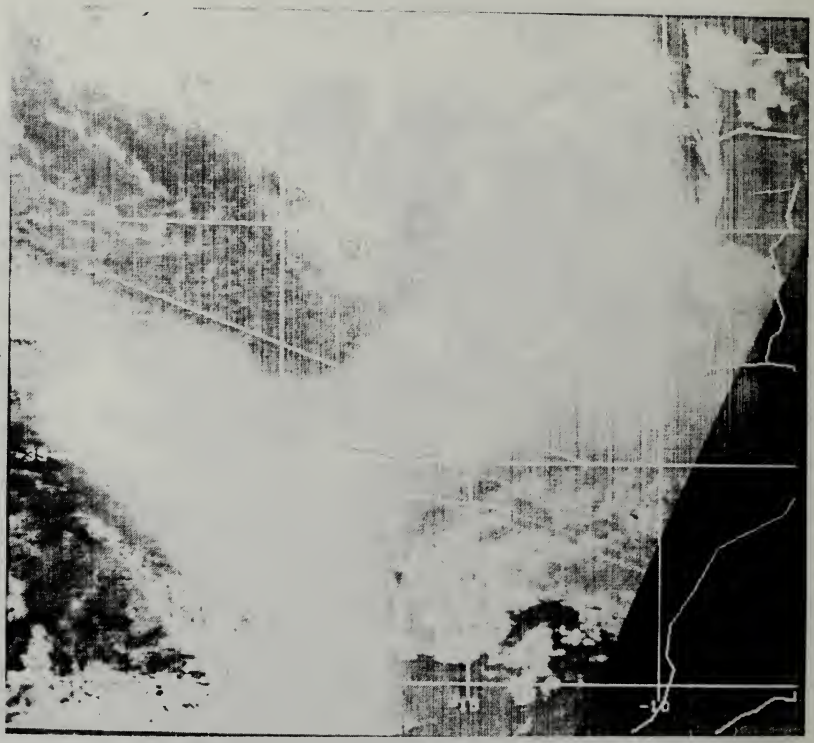

Figure 35a. LOW3 Satellite Image of 093900 UTC 17JUN92

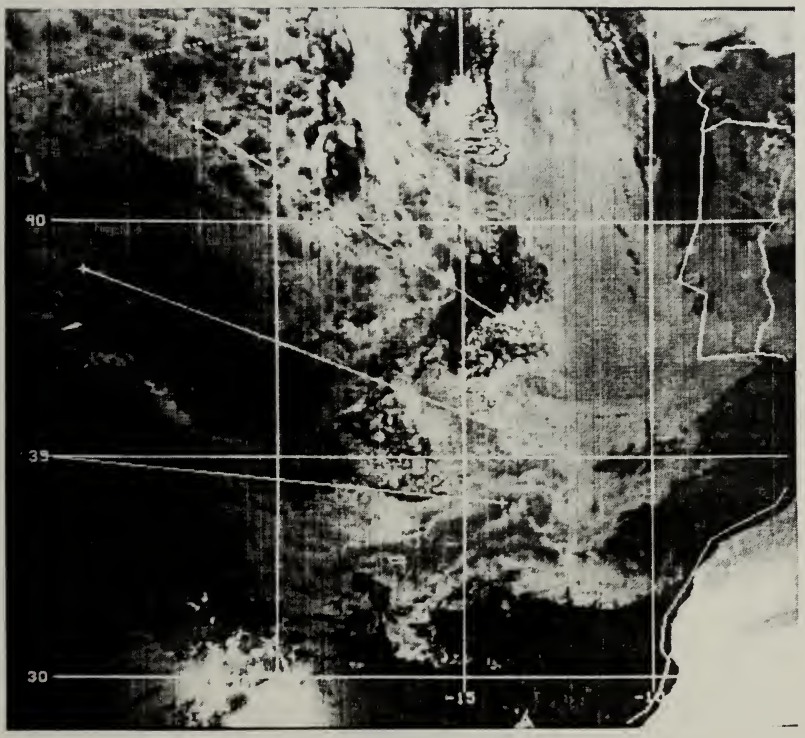

Figure 35b. LOW3 Satellite Image of 154930 UTC 17JUN92

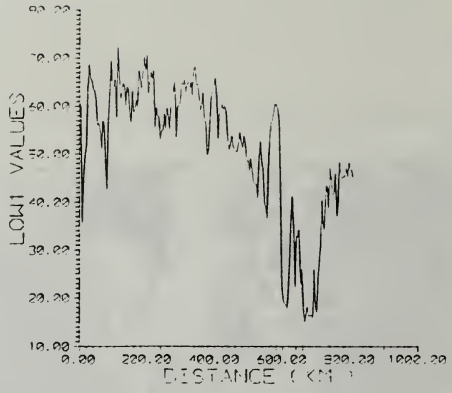

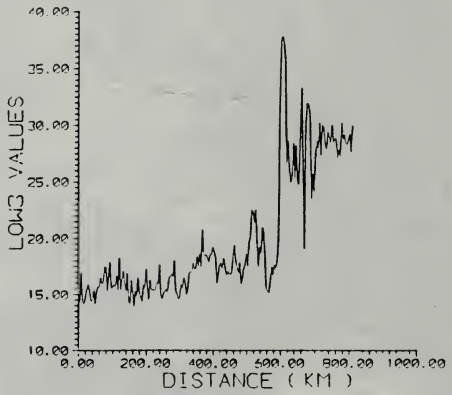

Figure 36. Parameter Results from 093900 UTC 17JUN92: Track A

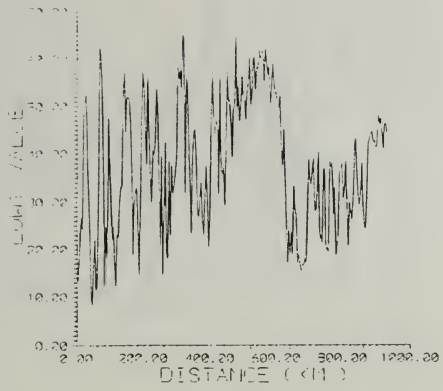

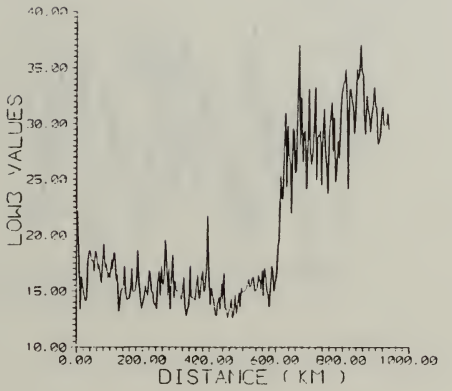

Figure 37. Parameter Results from 093900 UTC 17JUN92: Track B

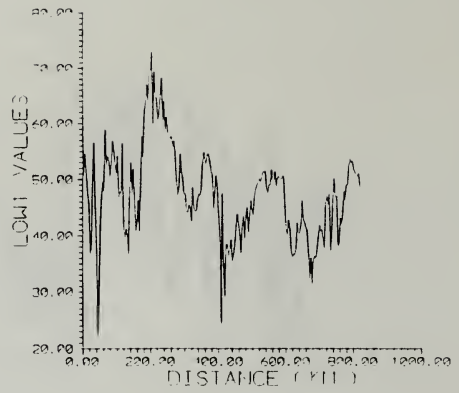

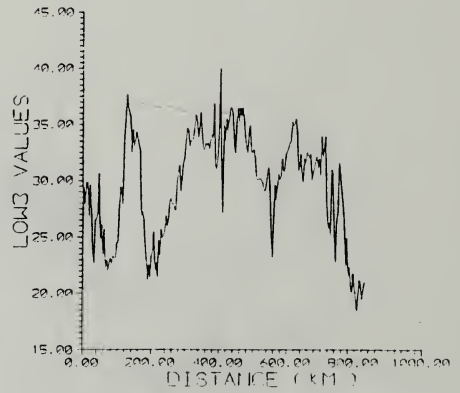

Figure 38. Parameter Results from 093900 UTC 17JUN92: Track C

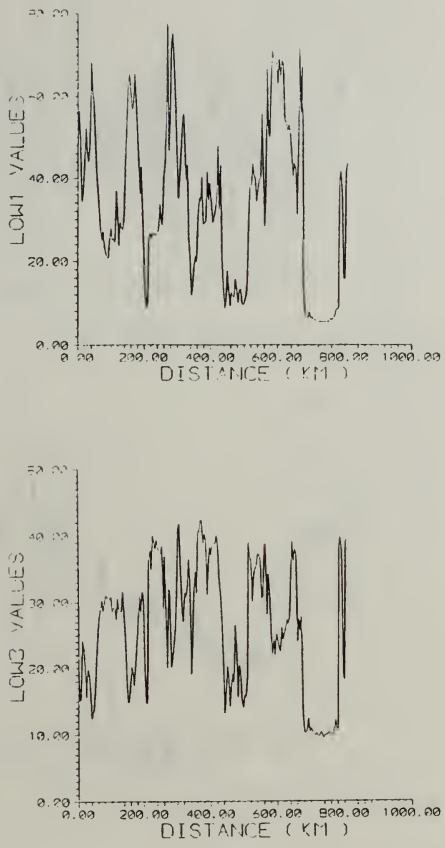

Figure 39. Parameter Results from 154930 UTC 17JUN92: Track A

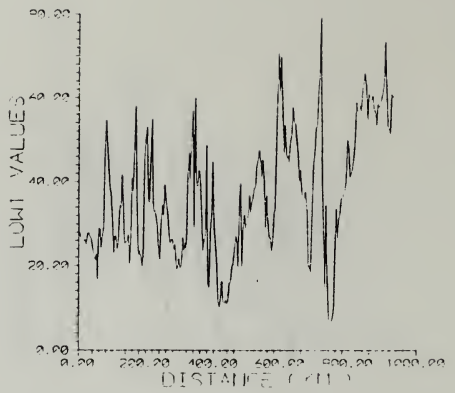

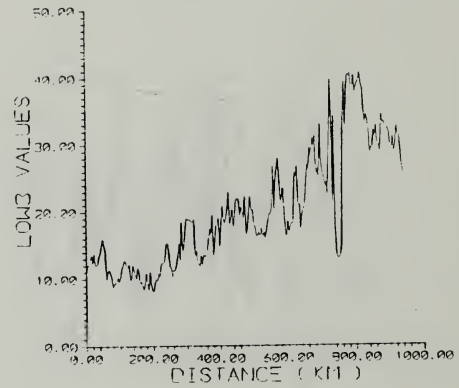

Figure 40. Parameter Results from 154930 UTC 17JUN92: Track B

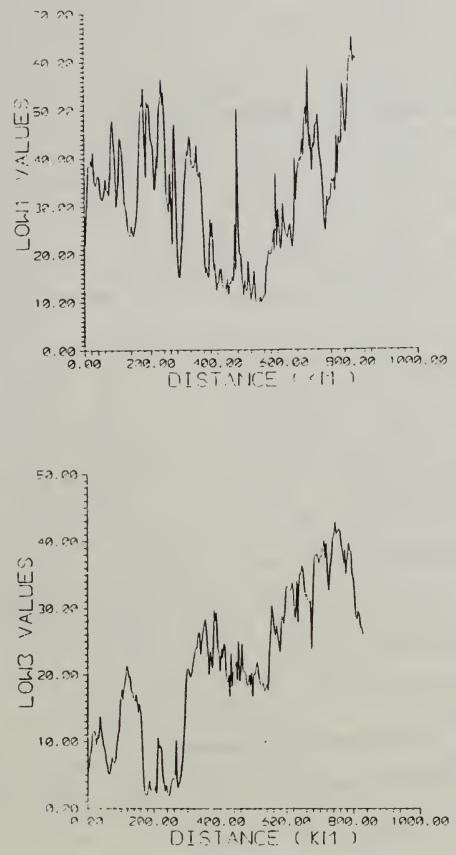

Figure 41. Parameter Results from 154930 UTC 17JUN92: Track C

the waters just south of the British Isles, while eastern region parcels originate from western France Bay of Biscay locations.

b. Satellite Interpretation

Figure 44 LOW1 image shows the maritime air mass consisting of a more reflective region in the northeast with cumuliform and stratocumuliform cloudiness. The region extending across the center of the image from the northwest to southeast corners is widely scattered with stratocumulus clouds. The continental air mass shows less reflective stratocumuliform cloudiness. Following the apparent motion of the clouds throughout the casy study sequence indicates that the southern region is the remnant of the continental air mass which originated off the Portuguese coast on June 14th.

Figure 45 LOW3 image shows a dominant cirrus shield in the southwest quadrant, with reflectances increasing in a northeastly direction across the image.

c. Cross-section Results

LOW3 imagery (Figure 45) indicates the lack of a cloud-free region and therefore, optical depth and S12 parameters are not addressed.

(1) LOW1

Figures 46 and 47 depict generally lower values of LOW1 overall as the regions depict less reflective cloudiness. LOW1 values are highest in thicker, highly

reflective areas i.e. scattered cloudiness along the tracks. Figure 46 depicts the expected higher LOW1 values characteristic of an overcast track, with the highest LOW1 values in the eastern portion of the continental air mass. (Note: The 0.00 LOW1 value in Figure 46 is due to bad satellite data points and should be disregarded).

(2) LOW3

Figure 46 shows that values uniformly decrease from 30 to approximately 8 west-to-east across the track. This is due to the transport of the continental air mass towards the northwest, bringing continental aerosol characteristics to the western portion of the image. Figures 47 and 48 show increasing LOW3 values west-to-east (.10 to .37 and .10 to .50 respectively), which indicate that the southern continental air mass is not strongly modified by the maritime environment on the eastern extreme of the project area. (Note: The spike in Figure 46 of LOW3 at approximately 500 km is due to bad satellite data points and should be disregarded).

B. CASE STUDY CONCLUSIONS

Aircraft data collected during ASTEX '92 confirmed aerosol plumes to be present within the air masses studied for this thesis. Specifically, Johnson and Taylor (1992) confirmed increased numbers in aerosol particles above the boundary layer (C-130 data) and Clarke (1992) confirmed increases in

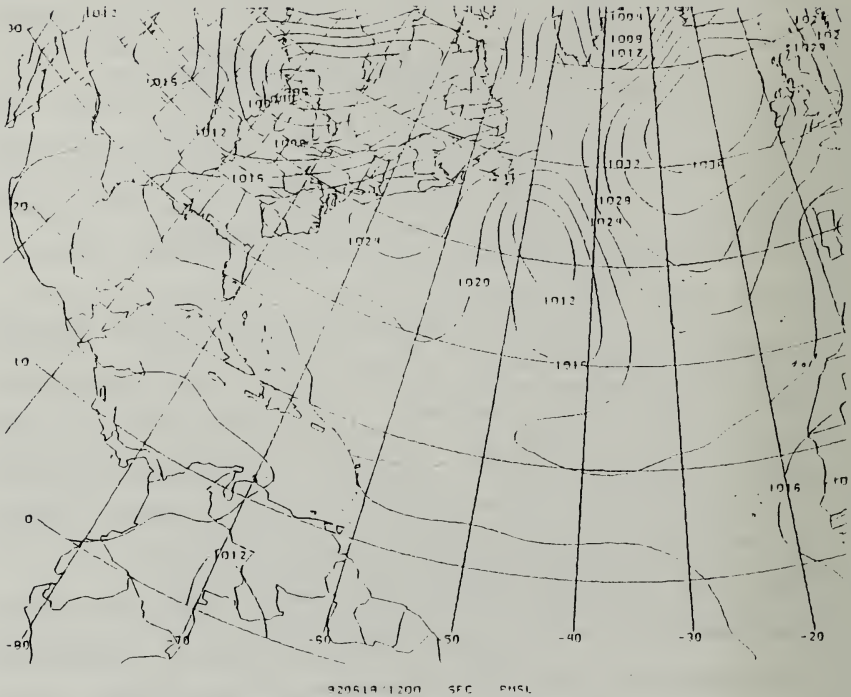

Figure 42. Surface Pressure Chart Valid 1200 UTC 18JUN92

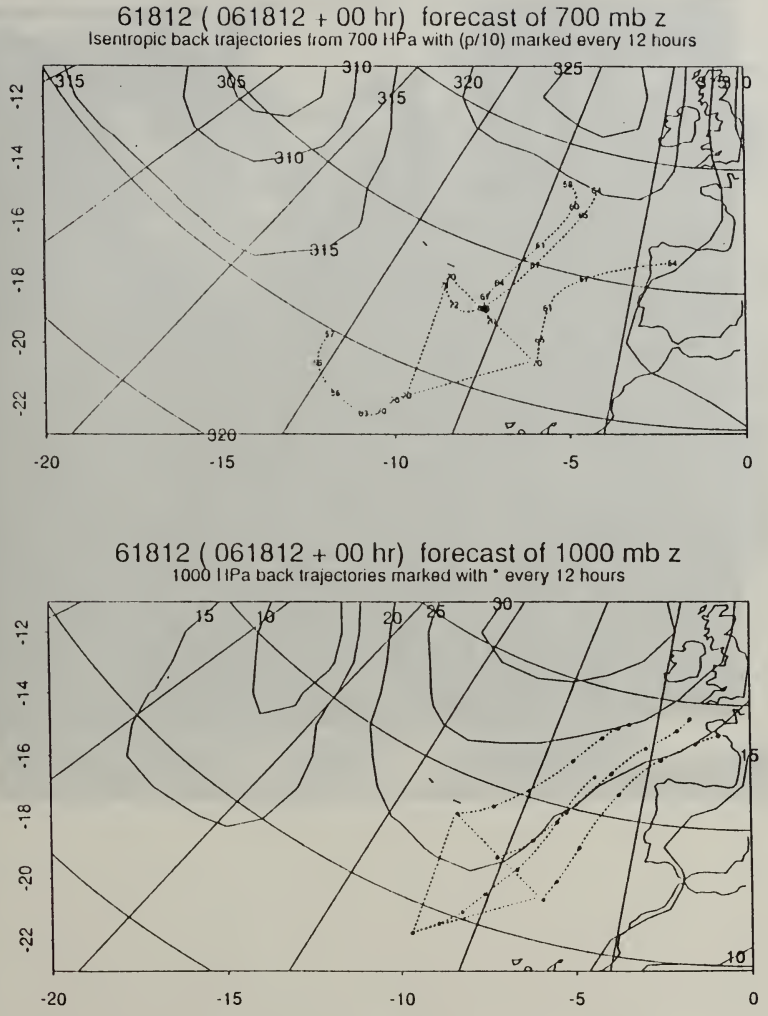

Figure 43. 18JUN92 Back Trajectories Within the Project Region: (a) 700mb and (b) 1000mb

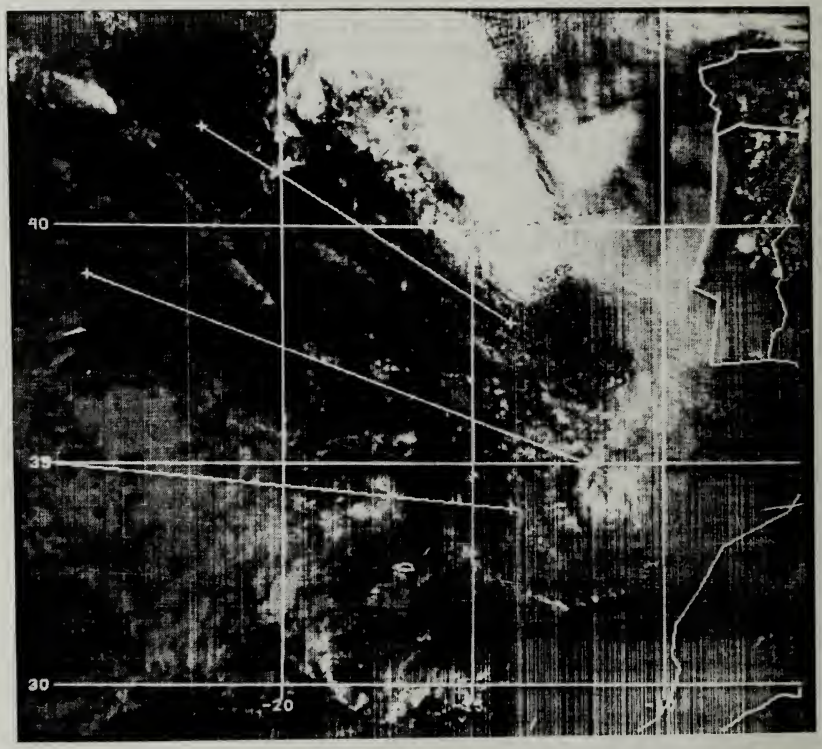

Figure 44. LOW1 Satellite Image of 153745 UTC 18JUN92

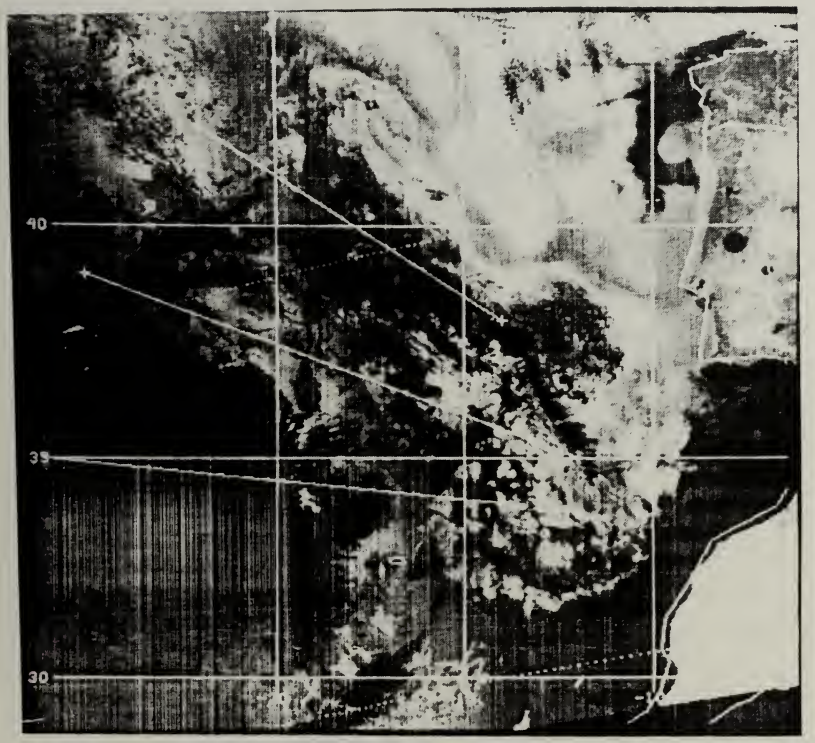

Figure 45. LOW3 Satellite Image of 153745 UTC 18JUN92

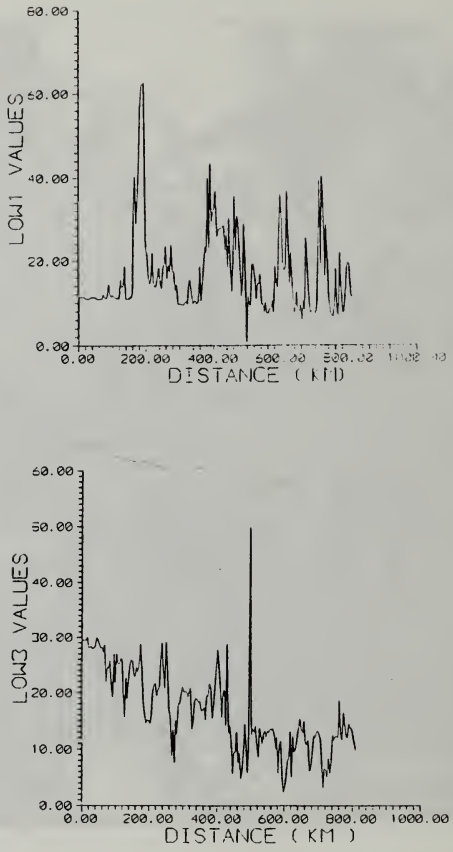

Figure 46. Parameter Results from 153745 UTC 18JUN92: Track A

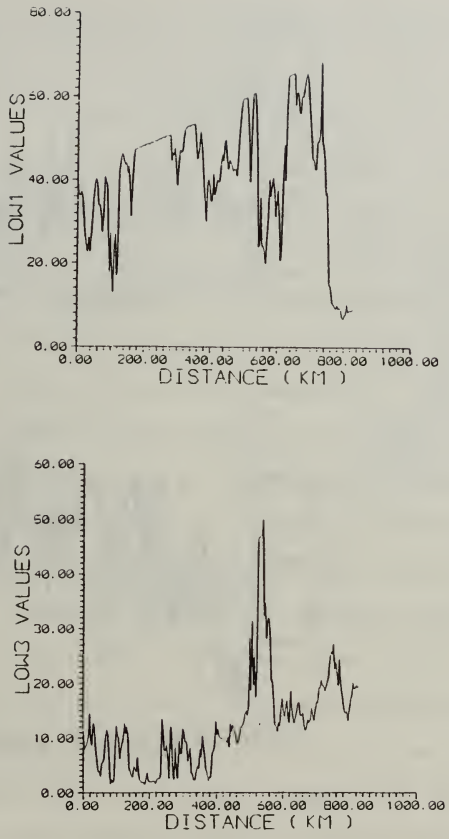

Figure 47. Parameter Results from 153745 UTC 18JUN92: Track B

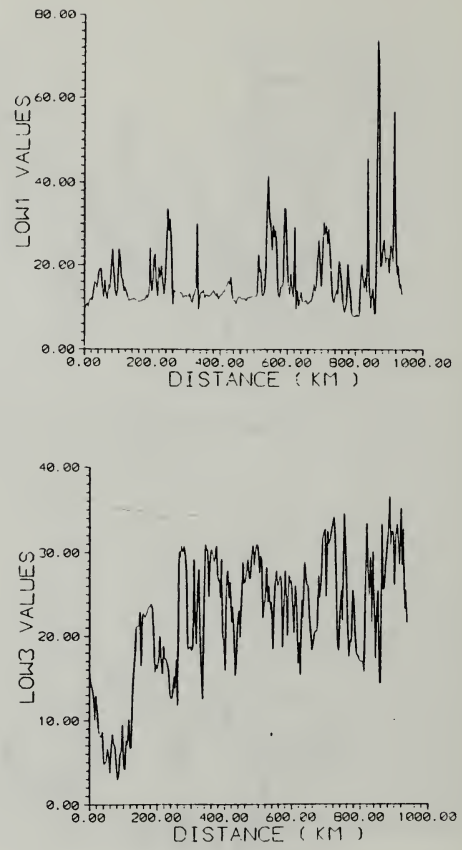

Figure 48. Parameter Results from 153745 UTC 18JUN92: Track C

mineral aerosols above the boundary layer (Electra aircraft data).

Parameter results verify the motions of continental and maritime air masses for the period of 14 - 18 June, 1992. Figure 49 shows the apparent motion of these air masses for the duration of the case study. Directions of motion were obtained through a combination of synoptic patterns, satellite imagery, and parameter results (optical depth, S12 values, LOW1, and LOW3). The south and westward motion of the continental air mass becomes apparent on 16 June on satellite imagery (Figures 24a, 24b, 25a, and 25b). The gradual northeastward movement of the maritime air mass and a more cellular cloud appearance is also supported by the imagery. In addition, the parameter values (especially optical depth, S12, and LOW3) reflect the motions of the two air masses. Figure 50 shows temporal changes of optical depth and S12 throughout the case study. It shows that, over time, as optical depth values increased, S12 values decreased. As previously mentioned, one interpretation is that increased optical depth indicates a greater number of aerosols; a decrease in S12 in conjunction with the optical depth increase would dictate that the additional aerosol particles would have to be larger than the existing ones within the air mass. This supports the addition of desert dust aerosol particles into the continental regime (Johnson and Taylor, 1992).

Figure 51 depicts the air mass values for LOW1 and LOW3 over time. LOW3 results indicate the additional droplets and the decrease in droplet radius present in the continental regime during later stages (16 - 18 June). LOW1 results in Figure 51 show the decline of the maritime thicknesses and cloud brightness and the increase in reflectivity of the continental regime. This supports the increase in aerosol content in the continental air mass throughout the study (as well as the loss of aerosols in the maritime region).

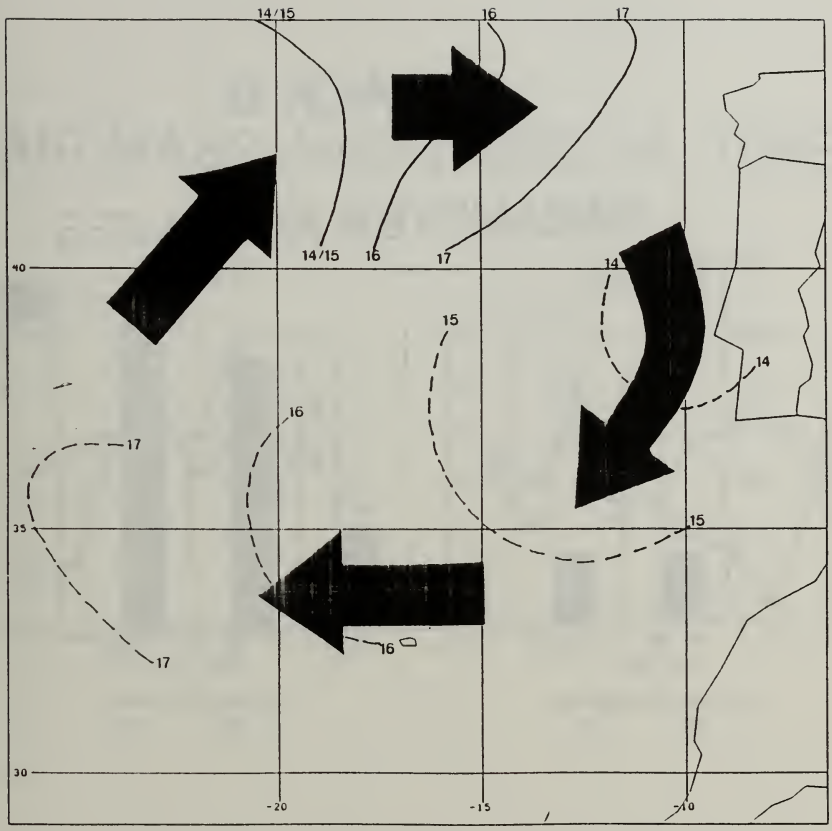

Figure 49. Continental (dashed) and Maritime (solid) Air Mass Motion for 14JUN92 - 17JUN92

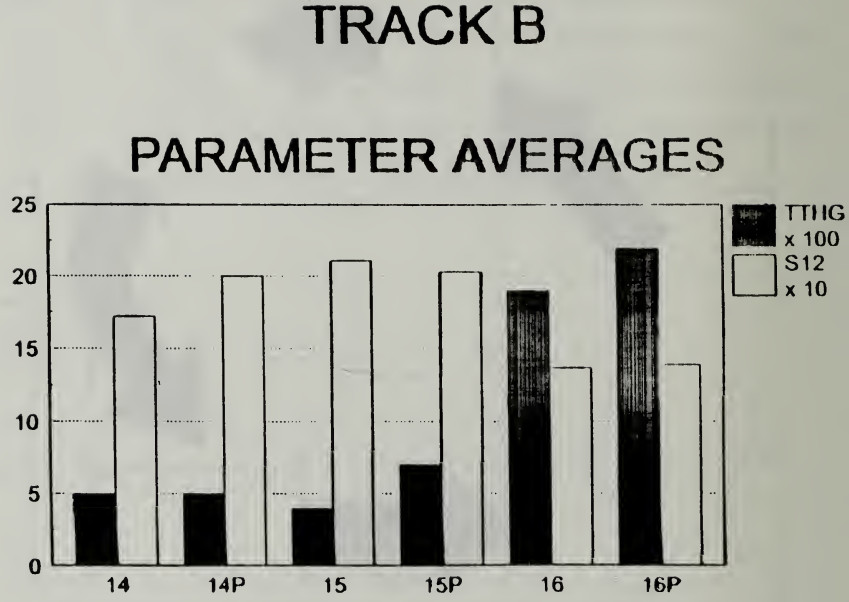

Figure 50. Average Optical Depth and S12 Value Plots
14JUN92 - 16JUN92

AIR MASS AVERAGES VS. TIME

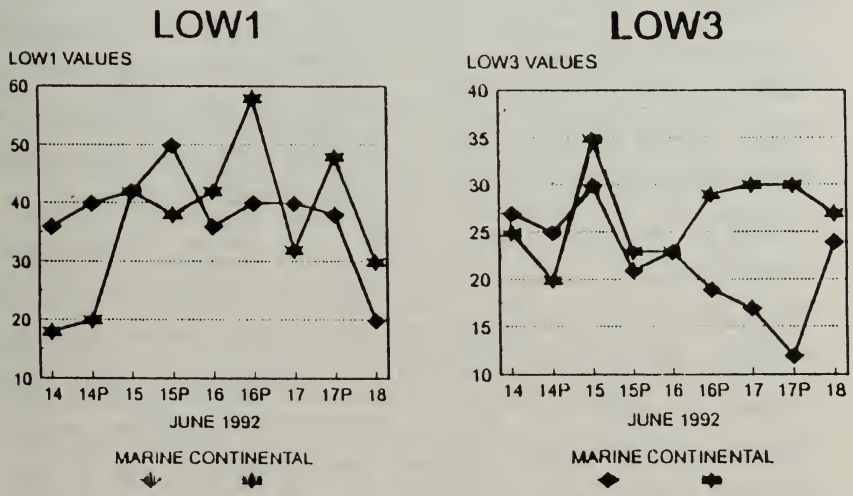

Figure 51. Marine versus Continental LOW1 and LOW3 Values 14JUN92 - 18JUN92

V. CONCLUSIONS AND RECOMMENDATIONS

A. CONCLUSIONS

This case study describes an ideal synoptic situation for qualitatively using satellite imagery to evaluate aerosols present within air masses and the subsequent interaction of continental and maritime aerosols with clouds. Combined parameter evaluations provide a method of discerning continental and marine aerosols present within an air mass, as well as an indication of the motion of the particles over time. These parameter values obtained from satellite imagery are consistent with aircraft data collected during ASTEX '92. Based on synoptic flow patterns, air parcel trajectories, known aerosol sources, and satellite interpretation, the motions of the continental and maritime air masses described (Figure 51) are quite realistic. Increases in LOW3 values (seen on CSD3, 4, and 5) substantiate higher aerosol concentration, higher droplet concentrations, and a shift towards smaller mean cloud drop radii (Mineart, 1988); optical depth increases indicate increases in aerosol radii and numbers within the continental air mass.

Identification of aerosol sources is achieved through a combination of back trajectories of air parcels, parameter evaluation, and aircraft measurements. Evaluations of optical

depth in conjunction with S12 show the influx of larger particles into the continental region (CSD1 and 2). The origin of the aerosol influx is then confirmed through back trajectory and aircraft data analysis. In addition, back trajectories at the surface and 700 mb plus aircraft information allows for evaluation of the marine atmospheric boundary layer, with continental aerosols interacting in the upper limits of the boundary layer and mixing with marine aerosols from lower boundary layer sources.

Parameter evaluations indicating high aerosol concentration corresponded to increased areal cloud coverage and cloud thicknesses. Specific cloud structure differences between continental and marine air masses are not generally apparent; however, during the period 14 - 18 June, 1992, the gradual increases in both areal cloud coverage and cloud intensity of the continental regime is observed. Spatial distribution of the continental air mass expands to the south and west (Figure 51), and cellular cloud elements increase throughout the period. In contrast, the maritime air mass begins on 14 June as an intense, bright cloud area with large areal coverage which decreases dramatically in both spatial and areal coverage from 15 - 18 June, 1992.

Although future studies will most certainly look into detailed quantitative analyses of aerosol types and interactions collected during ASTEX '92, this study provides an innovative "first look" into using synoptic analysis and

satellite interpretation as a stepping stone to subsequent research.

B. RECOMMENDATIONS

Future satellite imagery aerosol studies should include a cloud screening algorithm to provide a mechanism for masking clouds across selected tracks. This would provide more accurate optical depth values and improve the analysis technique. Also, composite summaries of satellite imagery parameters would highlight any inconsistencies in measured variables in the region.

Due to the recent conclusion of the ASTEX '92 project, raw data and preliminary scientific reports were not available for use in this study. However, future studies should incorporate particle size distribution data, soundings, marine boundary layer studies, optical depth measurements, etc. into the satellite imagery interpretation study of aerosols. This would substantiate results and conclusions from this initial study and enable a quantitative analysis of the continental and marine aerosols present in the sampled project area.

LIST OF REFERENCES

Bloembergen, N., C. K. Patel, and G. Pake (chairpersons), 1987: Science and technology of directed energy weapons. Report of the American Society Study Group, *Reviews of Modern Physics*, **59**, S1-S202.

Charlson, R.J., J. E. Lovelock, M. O. Andreae, and S. G. Warren, 1987: Oceanic phytoplankton, atmospheric sulphur, cloud albedo, and climate, *Nature*, **326**, 655-661.

Clarke, A., 1992: Personal communication.

Clifford, M.B., 1991: Effects of water vapor and anisotropic scattering on aerosol optical depth retrieval. Master's Thesis, Naval Postgraduate School, Monterey, CA, 1-39.

d'Almeida, G.A., P. Koepke, E. Shettle, 1991: *Atmospheric Aerosols: Global Climatology and Radiative Characteristics*, A. Deepak Publishing, Hampton, VA, 11-234.

Deepak, A., 1982: *Atmospheric Aerosols: Their Formation, Optical Properties, and Effects*, Spectrum Press, Hampton, VA, 1-109.

Durkee, P.A., 1984: The relationship between marine aerosol particles and satellite-detected radiance. PhD. Thesis, Colorado State University, Fort Collins, CO, US ISSN 0067-0340, 124pp.

Johnson, D., J. Taylor, 1992: Personal communication.

Kidwell, K. B., 1986: *Polar Orbiter Users Guide*, National Environmental Satellite Data and Information Service, Washington D.C., 120pp.

Lenoble, J., 1985: *Radiative transfer in Scattering and Absorbing Atmosphere: Standard Computational Procedures*. A. Deepak Publishing, Hampton, VA, 300pp.

McCormick, R. A., and J. H. Ludwig, 1967: Climate modification by atmospheric aerosols. *Science*, **156**, 1358-1359.

Miller, B.H., 1991: Improved aerosol optical depth and particle size index from satellite detected radiance.

Mineart, G.M., 1988: Multispectral satellite analysis of marine stratocumulus cloud microphysics. Master's Thesis, Naval Postgraduate School, Monterey, CA, 1-123.

NASA, 1990: *FIRE Phase II: ASTEX Implementation Plan*, 63pp.

INITIAL DISTRIBUTION LIST

		No. Copies
1.	Defense Technical Information Center Cameron Station Alexandria VA 22304-6145	2
2.	Library, Code 052 Naval Postgraduate School Monterey CA 93943-5002	2
3.	Chairman (Code OC/Co) Department of Oceanography Naval Postgraduate School Monterey, CA 93943-5000	1
4.	Chairman (Code MR/Hy) Department of Meteorology Naval Postgraduate School Monterey, CA 93943-5000	1
5.	Professor Philip A. Durkee (Code MR/De) Department of Meteorology Naval Postgraduate School Monterey, CA 93943-5000	5
6.	Professor Patricia M. Pauley (Code MR/Pa) Department of Meteorology Naval Postgraduate School Monterey, CA 93943-5000	1
7.	Doug Johnson Meteorological Research Flight Y46 Building Royal Aerospace Establishment Farnborough, HANTS GU14 6TD, UK	1
8.	Professor Chris Bretherton Applied Mathmatics, FS-20 University of Washington Seattle, WA 98195	1
9.	Karen M. Ruppe, LT, USNR 2110 Manlyn Rd. Richmond, VA 23229	1

E46-217

DUDLEY KNOX LIBRARY
NAVAL POSTGRADUATE SCHOOL
MONTEREY, CALIFORNIA 93943-5002

Thesis
R887 Ruppe
c.1 A maritime and continental aerosol-cloud interaction study from ASTEX '92.

Thesis
R887 Ruppe
c.1 A maritime and continental aerosol-cloud interaction study from ASTEX '92.

AMERICAN BINDERY

DUDLEY KNOX LIBRARY
3 2768 00018331 3